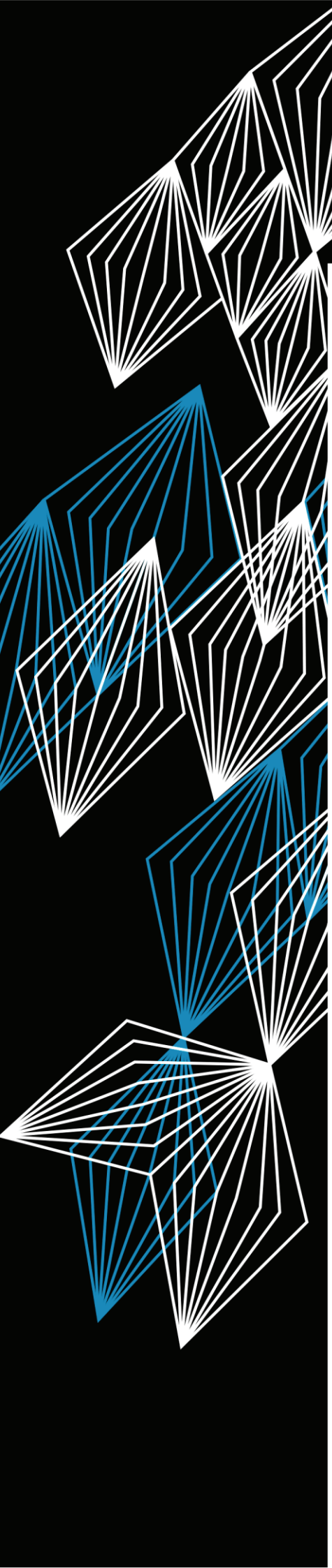

BACHELOR THESIS

Development of a Shape Memory Polymer-based Zigzag Structure by Magnetic Actuation

QUINTY VAN DER HELM

FACULTY OF ENGINEERING TECHNOLOGY

DEPARTMENT OF BIOMECHANICAL ENGINEERING

EXAMINATION COMMITTEE

PROF.DR. S. MISRA

DR.V. KALPATHY VENKITESWARAN

DR.IR.EP. HOUWMAN

DOCUMENT NUMBER

BE-902

UNIVERSITY OF TWENTE.

Thesis submitted by

Quinty van der Helm

under the supervision of

prof.dr. S. Misra,

dr.V. Kalpathy Venkiteswaran, and

dr.ir.EP. Houwman

in order to fulfill the necessary requirements to obtain a Bachelor's degree in

Biomechanical Engineering at the University of Twente

and defended on

Thursday, 24th of November, 2022

Abstract

Invasive techniques are widely used in clinical applications, however, this brings high risks in patient safety and post operative complications. Shape memory polymers (SMP) have come forward as a promising solution, but challenges are the recovery and steerability of the material used during Minimally Invasive Surgery (MIS). Controllability of SMP-based origami structures by magnetic actuation seems like a favorable solution due to its ability of retrieving large macroscopic changes. However, the influence of magnetic field strength and orientation needs to be tested to see if the SMP material has the ability to deform beyond its permanent and temporary structure and can therefore be used as a drug delivery system.

The ultimate goal of this research is to investigate the influence of strength and orientation of magnetic actuation on an SMP-based origami structure to determine whether it is possible to create a third configuration, the zigzag shape. During this study multiple steps are taken to reach this final goal. Starting off, multiple samples of SMP with grafted hinges are made in the lab. After doing some basic setup experiments on a one panel SMP plate, the influence of magnetic field strength and orientation is tested. From the results it can be concluded that when the magnet dipole moment is oriented perpendicular to the applied external field it will rotate both ways at a limited maximal rotational angle. Magnets with the dipole aligned to the external magnetic field can reach higher rotational angles after a threshold of about 15-25 mT is reached. However, the concept of 'perfect misalignment' is not taken into account here. The two panel experiments elaborate on the results of the one panel experiments by testing the possibility to create a V shape. In this setup, multiple ratios in dipole moment of two different magnets are tested, supported with calculations. From the results it can be observed that it is possible to create a V shape with alternating magnetic dipole moment vectors when they have a minimal value of 57.35×10^3 Am^2. During the last step, aimed at creating a zigzag shape, the two panel experiments are extended to four panel experiments. However, due to internal interactions of the magnets it is harder to realize such shapes in larger samples and the right combination for creating an actual zigzag shape has not been found yet.

Contents

1 Introduction

Invasive techniques are widely used in clinical applications, however these bring high risks in patient safety and post operative complications. In abdominal surgery, for example, limitations to manual surgical methods are human hand tremors, fatigue, vision of target location and inconvenient tool control (1). Because of this there has been a shift towards minimally invasive surgery (MIS). One of the key aspects of MIS is that it can be applied in limited space and field of vision without hand-eye coordination of the surgeon (2). The challenge in designing such a tool is that the size needs to be minimized without compromising its function. Shape memory polymer (SMP) has come forward as a promising solution, but challenges are the recovery to the permanent state and steerability of the material used during MIS. Control of SMP-based origami structures by magnetic actuation is a possible solution due to the possibility to achieve large macroscopic changes in restricted space without being harmful to humans (1). However the influence of magnetic field steering by changing field strength and orientation needs to be investigated to see if the SMP material can be deformed beyond its permanent and temporary structure and can therefore be used as a drug delivery system.

Considering the two requirements for an ideal drug delivery system, delivering the minimum sufficient amount of drugs to the target location for a therapeutic effect and delivering the drug with most advantageous kinetics to minimize unwanted side effects and optimize its beneficial response, SMP-based origami structures as drug delivery systems are considered to be a promising solution (3). Origami, oru-kami, literally stands for fold and paper (4). Although it can be seen as a form of art it has enormous potential in the medical world. Origami structures can take all kinds of shapes and sizes, just by folding. This allows for the the origami structure to transform from a functional state to a compact form, useful for transportation or storage. In medical procedures like minimally invasive surgery an origami-based medical device could easily travel through the body to previously inaccessible areas, by only making a small incision, and then take its functional form at its targeted location (5). Minimally invasive surgeries like these will minimize risks in patient safety, postoperative complications and improve recovery rate. One example of a successful origami drug delivery system was a device based on self-folding hydrogels by He et al. (4).

A material that also has self-folding properties is the, earlier mentioned, shape memory polymer (SMP). The main characteristic of SMP is that it is a dual-shape material which can show a plastic deformation to a temporary state when an external stimulus like heat is applied, but can thereafter return to its original shape when it is cooled down. This is also known as 'shape memory effect'(SME) (6). Advantages of SMP material are their tailored stiffness due to a wide range of glass transition temperatures, low costs because they are easy to process, biodegradability, high elastic deformation and low density (6). SMP has a variety of applications like engine parts, electronic parts, clothing, packaging, all types of equipment and also increasingly within the medical field. Common examples of SMP within the biomedical field are intravascular stents, aneurysm treatment, clot removal and drug delivery devices (6). SMP can be activated by different stimuli; thermal activation, solvent-induced recovery, light-induced recovery or can be mechanically driven (7). Each has its pros and cons dependent on the desired application. Due to the fact that drug delivery will take place in the body this research will focus on an SMP that is polyurethane-based with a (glass) transition temperature of 37 degrees Celsius so that it can unfold in the body without any extra required stimulus.

Another challenge that comes with drug delivery systems is the recovery and steerability of the device. Since magnetic actuators can be driven wirelessly by a magnetic field, magnetic actuation has been considered a promising technique for medical robots (8). It can both provide the needed power and accuracy that miniaturized applications need. Magnetically-actuated robots are applicable for a variety of minimally invasive surgical procedures throughout many regions of the body, including diagnostic imaging, implants, drug delivery and biopsy. Magnetic drug delivery has the advantage of being able to deliver the drugs to the site of disease without effecting other, healthy tissues and organs.

To optimize the steerability and controllability of a drug delivery system, in this case an SMP-based origami structure, different aspects need to be examined. First of all the SMP material needs to be able to deform beyond its two states, the permanent and temporary state, to take on its function form at a targeted location. Next, the magnetic fields need to be strong enough to be able to deform the material in the most optimal way without being dangerous for the patient in question. Furthermore, the body has a complex structure through which the drug delivery system needs to travel and eventually perform its function. Therefore it is essential to investigate from what orientation the origami structure will be able to deform to the desired shape in the shortest amount of time, being able to deliver the drugs to the correct area.

The research presented in this report focuses on the influence of strength and orientation of magnetic actuation on a SMP-based origami structure. The ultimate goal is to investigate if this method makes it possible to create a third configuration, the zigzag shape. In earlier studies (9) (10) it was concluded that SMP samples can recover fully and even result in over-bending when applying the correct magnetic field. From COMSOL computations it was however concluded that the zigzag shape was harder to realize. After conducting literature research, multiple calculations and experiments on the influence of magnetic field strength and orientation, these results and observations will be used to find improved operating conditions for which the SMP-based origami structure will deform beyond its two states, in this case a zigzag form.

In short, at the start of this research SMP will be made within the lab, combining different protocols to produce a uniform sheet. Next, hinges will be engraved to the right dimensions in the multiple paneled structure. After doing some basic setup experiments during the one panel analysis, the influence of magnetic field strength and orientation is tested. By changing the current running through the magnetic field coils and testing different magnets, the influence of magnetic field strength will become clear. To determine the influence of orientation, the direction of the field will be adjusted. Using these results an attempt will be made to create a V shape out 2 panels, testing the ratio of magnetic dipole strength. And finally the two panel experiments will be elaborated to see if it is possible to create a third configuration, the zigzag shape, during the four panel experiments.

2 Theoretical Background

2.1 Origami

Origami is a traditional art form in which real-life figures are created by folding uncut sheets of paper. Crease patterns, i.e. the arrangement of folding lines to create geometrical patterns, uniquely define the resulting origami structure. A crease is a line along which a fold takes place, also known as a hinge, and this is where bending of the sheet occurs. The panels surrounding the hinges, are made of stiff material and form the main structure in an origami device. There are two types of folds that can be defined within origami, mountain folds and valley folds as seen in figure 1. In the figure the mountain folds faces upwards and occurs when the crease is convex and has an angle between 0 and -180 degrees. A valley fold moves in the opposite direction, concave, and has a crease angle between 0 and +180 degrees[1].

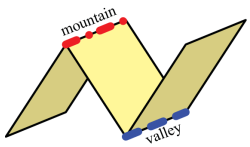

Figure 1: Mountain and Valley folds in origami. The red dotted line represents the mountain fold in convex and the blue line the valley fold in concave.

Key aspects, making origami appealing for engineering applications are: deployability, scalability, self-actuation, reconfigurability, tunability and easiness in manufacturing (11). Deployability gives the origami structure the capability to deploy from an initial 2D configuration to a 3D final state, which is useful within minimally invasive surgery (MIS) as was suggested in the previous section. Another property that is useful within MIS is scalability. Origami-based designs can range from micro to macro scale and are therefore scale independent. The property self-actuation indicates that the design is able to deploy without external actuators, however this will not be the case within this study. Reconfigurability indicates that when one crease pattern is altered it could change the 3D configuration of an origami-based design without further geometrical alterations. This is useful when the design needs to dynamically change due to a specific design constraint. Furthermore, origami-based designs can be tailored for specific tasks by changing their geometrical properties. This can be defined as tunability. Last but not least, the advantage in manufacturing origami-based designs is their capability to be assembled in final 3D configurations by using 2D parts. All these properties are key aspects of origami-based designs to have a wide range of possible applications.

2.2 Shape Memory Polymers

2.2.1 General

Shape Memory Poymers (SMP) are dual-shape materials that can change from a temporary state (A) back to its permanent state (B) by some kind of stimulus like light or heat. Because the shape-memory effect is dependent on the molecular architecture and not its chemical structure, this material does not have fixed mechanical properties, but can be adjusted to fit specific applications (12). Mechanical properties are greatly effected by the arrangement of internal structure and not by their chemical composition. This explains the wide range of distinctive SMP types and possible implementation in various areas.

SMP 3D structures can be made by conventional methods like extrusion or molding. The polymer is then formed in its permanent shape B. Thereafter the SMP material is deformed to its temporary

[1]The angle is defined as positive for counter-clockwise bending of the right panel with respect to the panel to the left of the crease.

state A using a mechanical force, often at an elevated temperature, in a stage called programming. When a specific external stimulus is applied, the polymer recovers to its initial permanent shape B. This process is called recovery. Within this one-way memory shape cycle, there is also a phase in between the programming and the recovery states called storage. This is when the temporary shape is locked by cooling the SMP below the activation (glass) temperature and the removal of the mechanical force. This whole one-way memory shape cycle is illustrated in figure 2.

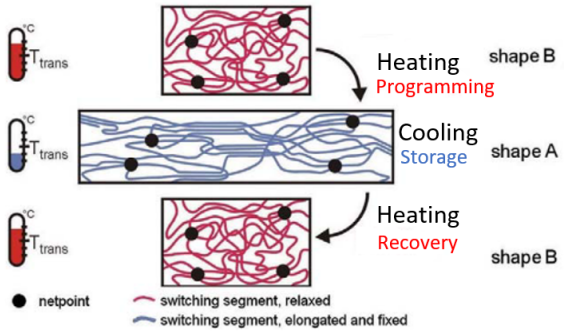

Figure 2: One-way thermally induced memory shape cycle. (13). The states in which the SMP exists is indicated by programming, storage and recovery.

The ability of SMPs to memorize its original permanent shape is due to the cross-links between the molecules which are part of the structure. Between these cross-links are switching segments that undergo the reversible shape change when an external stimulus is applied. Above a certain (glass) transition temperature the polymer chains of the switching segments become highly flexible and can therefor easily deform at low stresses. When the temperature is lowered the polymer chains will lock in the temporary state, limiting possible deformation. When the material is constrained during its recovery phase, it will apply a kinetic force instead of recovering its original shape (13).

2.2.2 DiAPLEX

DiAPLEX is a commercially available SMP material made from polyurethane. This is a common material with thermomechanical behavior and shape memory properties like ethylene-vinyl acetate copolymers, oligo(ε-caprolactones), poly(ethylene glycol), and poly(ethylene terephthalates) do (14). SMP can take on different configurations based on its material type. Both MM which is a material made out of pellets and MB that is made of microbeads are dry materials. MM is molded by extrusion or injection, whereas no information is given on MB by the manufacturer leading to disregard of this fact. MP consists of an equal mixture of Resin (A) and a Hardener (B), which are potted in separate storage containers. In this research type MP is used.
DiAPLEX has four principal properties that lead to distinctive SMP types. (1) The elastic modulus property, which describes the resistance of a substance to deform elastically. Its glass transition temperature (Tg) can be tuned in the range from -40 to +90 degrees Celsius. The elastic modulus changes substantially around this glass transition temperature, staying constant beyond this center point as can be seen in figure 3. However, all SMP types have the same elastic modulus below the glass transition temperature but not above it. The lower the glass transition temperature, the larger the change in elastic modulus.

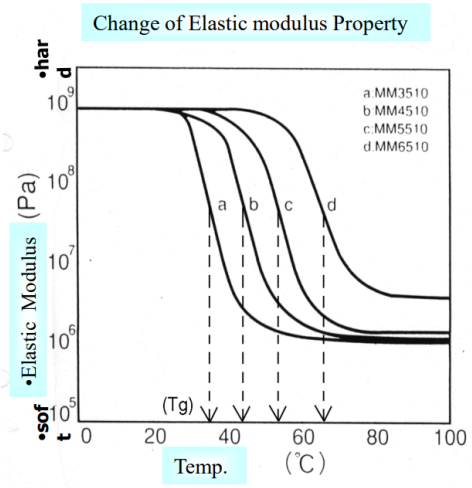

Figure 3: Change in elastic modulus of a few DiAPLEX compounds around Tg(15).

As also can be seen in figure 3 there is one compound with a glass transition temperature close to the temperature of the human body, around 37 degrees Celsius, therefore this compound type (MP-3510) will be used in the present research. (2) The second property is shape recovery and rigidation, which explains the one-way memory shape cycle like mentioned above. (3) DiAPLEX's third property is energy dissipation, this is when energy transforms from its initial state to a final state without having the capability to convert back to its original form. This factor in the transition region is very similar to that of human skin, providing tactility. (4) And last but not least, the gas permeability property of DiAPLEX membrane. It has a large moisture permeability above Tg but low below (15). Water absorbed in SMP can be split into two parts, namely, free water and bound water. Bound water, due to moisture permeability, reduces the glass transition temperature almost linearly and has influence on the uniaxial tensile behavior of SMP while the effects of free water are negligible (16).

2.3 Magnetic Actuation

As can be concluded from the paragraph above, SMP is able to exist in a flexible state. When this state is reached, magnetic actuation can be used to control the material and influence the shape it will adopt when cooled down below the glass transition temperature. Magnetic actuation is a promising technique because of the possibility of providing precise control and the required force to guide robotic devices in miniaturized applications (8). Magnetically-actuated miniature robotic devices are not harmful to humans and can be used in small, restricted spaces (17). Therefore they are being developed for many different areas of minimally invasive surgery and diagnostics. This ranges from the abdomen, heart and brain to the eye, ear, and vascular system. Within these different regions they can operate in several ways such as diagnostic imaging, as implants, for drug delivery or for taking a biopsy (8).

Magnetic actuation is achieved by 'imparting force and/or torque on magnetic objects embedded with magnets or made of magnetizable materials through remotely applied magnetic fields (18)'. In other words, magnetic actuation is based on the interaction forces of magnetic fields on (small) permanent magnets. When a magnetic object is subjected to a magnetic field, it experiences a magnetic force F_m and a torque T_m which are expressed in the following equations.

$$F_m = \int_V (M \cdot \nabla B) dV \tag{1}$$

$$T_m = \int_V (M \times B) dV \tag{2}$$

Here M is the internal magnetization per unit volume, B is the magnetic flux density and V is the volume of the magnetic material. When dimensions of the magnetic object are relatively small the internal magnetization is concentrated in one point, so B and ∇B can be assumed constant. When the volume integral only extends over the magnetization, this results in a magnetic moment m. Therefore the equations mentioned above can be simplified to,

$$\vec{F_m} = \vec{m} \cdot \nabla \vec{B} \tag{3}$$

$$\vec{T_m} = \vec{m} \times \vec{B} \tag{4}$$

As can be seen in the above equations, the magnetic force is proportional to the gradient of the external magnetic field at the position of the magnet m, and the magnetic torque is equal to the cross product of the magnetic moment vector and the magnetic flux density vector. This explains the fact that magnetic torque tends to align the magnetic moment vectors parallel to the external magnetic field direction (19). The mechanical force moves the magnet in the increasing field gradient direction and can therefore result in deformation.

The actuating field for magnetic soft robots can be generated using permanent magnets or electromagnetic coils. Both methods have advantages and disadvantages. Permanent magnets can create strong, constant fields and actuation can only be achieved by precise orientation and positioning of the external magnets. The field magnitude however can be adjusted in electromagnetic coils by tuning the coil current, leading to more degrees of freedom. The only problem with these coils is heating and scallibility when applied for manipulation of origami structures in larger objects, like the human body (20). In this research a device with three paired coil sets, will be used which has a orthogonal distribution due to the coupled electromagnets, and a workspace in the central position. The most common type is the multi-axial Helmholtz coil. This type of system can generate arbitrary oriented strong magnetic fields with high uniformity in a plane (two Helmholtz pairs) or volume (three Helmholtz pairs) (8). In this research the multi-axial Helmholtz coil is known as PagMag (21). The Helmholtz coil magnetic field equation is given as,

$$B = \frac{0.8991 \times 1010^{-6} nI}{r} \tag{5}$$

Equation 5 shows that a smaller radius generates a stronger magnetic field density, as does the number of turns (22). To still generate large torques for the relatively small magnetic field that can be obtained with a usual laboratory Helmholtz coil it is beneficial to have a net moment μ as large as possible.

2.4 Calculations

2.4.1 One Panel Analysis

To understand magnetic actuation of origami structures it is essential to analyse factors leading to the rotation of a single origami panel. In previous research, this analysis has been partly conducted, and will therefore be used as a stepping stone in this study. In figure 4 a modified sketch of the single panel set-up that was used in the thesis of Sanne Cox (9) is shown.

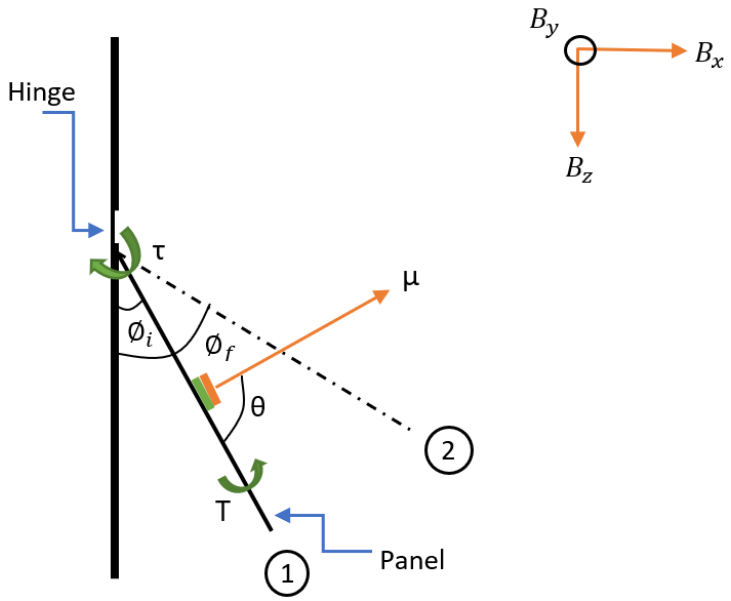

Figure 4: Single panel setup, with the first panel fixed. In this case the panel is already rotated to an initial starting point with a rotational angle ϕ_i. The red block indicates the north-pole of the magnet while green is the south-pole. Because the magnetic vector μ ventures to align with the applied magnetic field B, the panel rotates from point 1 to point 2. The moment τ is induced by the stiffness of the hinge.

In the case depicted in figure 4, the panel had a centered magnetic dipole moment μ oriented perpendicular to the panel. To try and rotate the panel from position 1 to position 2 the magnetic vector μ ventures to align with the applied magnetic field B. To achieve any movement, this moment needs to be greater than the moment τ induced by the stiffness of the hinge. When the magnetic torque and the moment due to stiffness are in equilibrium, the motion will stop. The moment balance describing the situation in figure 4 is dependent on multiple factors. The moment balance is described in equation 6.

$$\sum M = \vec{T_m} - \vec{\tau} \tag{6}$$

In this case no force will be applied on the SMP material. This is because the magnetic field gradient is almost equal to zero in a Helmholtz coil, considering that the field is uniform throughout, resulting in a magnetic force of zero in equation 3. Also, because all motions occur within a plane, all equations will be denoted by scalars. One aspect that needs be considered is the rotational stiffness K about the hinge which can be described as the ratio of applied moment to the angle of rotation. The internal moment of the hinge, when the panel moves from angle ϕ_i to ϕ_f, can be described as

$$\tau = -K(\phi_f - \phi_i) \tag{7}$$

Filling in equations 4 and 7 in the moment balance 6 gives,

$$\mu B \sin \phi_i - (K(\phi_f - \phi_i)) = 0 \tag{8}$$

Considering that a permanent magnet will be placed on the panel, its magnetic dipole moment can be calculated with the following equation.

$$\mu = \frac{V \cdot B_r}{\mu_0} \tag{9}$$

V is the volume of the magnet, B_r is the residual flux density and μ_0 is the permeability of vacuum, with a constant value of $4\pi \cdot 10^{-7}$ N/A^2.

The bending stiffness of the hinge can be calculated by filling in its geometry in formula 10.

$$K = \frac{EI}{L} \tag{10}$$

E is the Young's modulus of the material, I is the moment of inertia and L the length of the hinge. The width, length and height of the hinge stays constant throughout all the experiments. In case of DiAPLEX MP-3510 the Young's modulus, also known as the 100% modulus in the rubber phase, has a given value of 8.0 MPa. The formula for calculating the moment of inertia of a rectangular cross section is,

$$I = \frac{bh^3}{12} \tag{11}$$

In figure 5 is indicated what the length, width and height in these calculation comprise, providing this research.

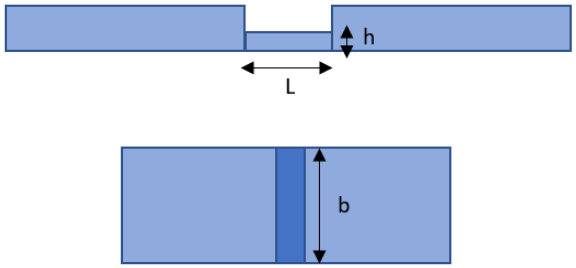

Figure 5: Hinge dimensions indicated with b, L and h. b is the width of the hinge, L the length and h the height.

2.4.2 Two Panel Analysis

To be able to create a zigzag shape multiple magnets will be placed on various panels. However to approximate the magnet ratio that is needed to obtain the desired bending angle, a two panel analysis is conducted. In figure 6 a sketch is given of the two panel setup with all considerable factors.

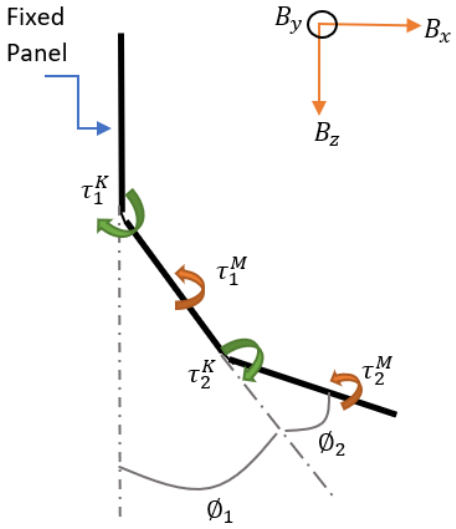

Figure 6: Two panel setup, with a fixed first panel. The internal moment of hinge number one and two are given in green, while the torque, due to the dipole moment that ventures to align with the applied magnetic field, is given in red for the two rotating panels. The rotational angles of the first and second hinge are indicated with ϕ_1 and ϕ_2, respectively.

To be able to calculate τ^M of panels 1 and 2 the angle between the magnetic dipole and the outer magnetic field is needed. In figure 7 the magnet placement on each of the panels can be seen and the direction of their magnetic dipole.

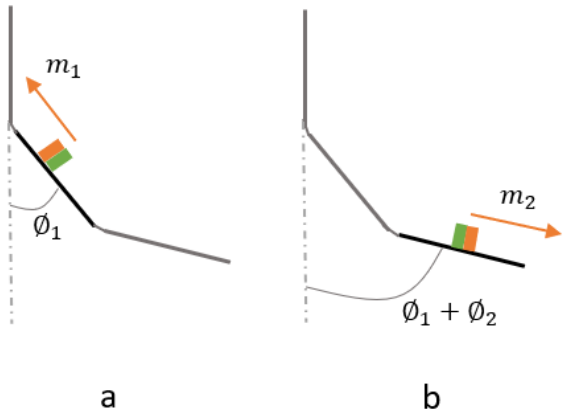

Figure 7: Two panel setup, with a fixed first panel. In a, the magnet placement on the first panel with the corresponding magnetic dipole direction is given as well as the rotational angle ϕ_1. In b, the magnet placement on the second panel is given with the corresponding magnetic dipole direction and the total rotational angle denoted by $\phi_1+\phi_2$.

From the figure it can be concluded that the τ_1^M and τ_2^M can be calculated as follows when the external field is oriented in the positive x-direction,

$$\tau_1^M = m_1 B \sin(90° + \phi_1) \tag{12}$$

$$\tau_2^M = m_2 B \sin(90° - (\phi_1 + \phi_2)) \tag{13}$$

while τ_1^K and τ_2^K can be denoted as,

$$\tau_1^K = K\phi_1 \tag{14}$$

$$\tau_2^K = K\phi_2 \tag{15}$$

A two panel set-up can be split up in two separate free body diagrams as portrayed in figure 8.

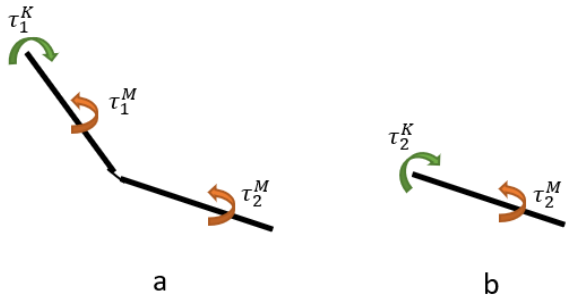

Figure 8: Two panel setup, with a fixed first panel. In a, the free body diagram of the first panel is given. In b, the free body diagram of the second panel is given.

The equations that correspond to the free body diagrams given in figure 8 are,

$$\tau_1^K = \tau_1^M + \tau_2^M \tag{16}$$

$$\tau_2^K = \tau_2^M \tag{17}$$

As can be seen in the above equations is τ_2^K equal to τ_2^M and can therefore be substituted in equation 16 resulting in,

$$\tau_1^K = \tau_1^M + \tau_2^K \tag{18}$$

Filling in equations 12 and 13 while simplifying $\sin(90)$ to cosine gives,

$$K\phi_1 = m_1 B \cos(\phi_1) + K\phi_2 \tag{19}$$

$$K\phi_2 = m_2 B \cos(\phi_1 + \phi_2) \tag{20}$$

With this derivation multiple parameters can be investigated like the angle at specific magnet ratios.

3 Preparation

In this section an overview is given of all the steps that need to take place before the experiments provided in this study can be conducted. These are: i) the Gauss meter experiment, ii) the fabrication of SMP sheets and iii) the setup. It is important to see what the setup should be and to confirm that the correct magnetic field is being produced at the desired location. This is done with a Tesla (Gauss) meter experiment. Also, clean sheets of SMP need to be made with the desired elastic behavior when conducting experiments. All these elements will be explained in the following sections.

3.1 Gauss Meter Experiment

3.1.1 Background and methodology

In this experiment the magnetic field strength B running throughout the outer two Helmholtz coils will be measured in the x- and z- direction, which are the two field orientations used in this study. This is to determine the influence of position and orientation within the coils and to confirm that the desired magnetic field strength is reached. This experiment is conducted with a Gauss meter, which is also called a Tesla meter when one needs to measure stronger fields. The Gauss meter works on the principle of the Hall effect. The Hall effect explains that when a current passes through a conductor, the magnetic force will 'push' electrons to one side, creating a measurable voltage due to the charge dis-balance. The voltage is directly proportionate to the magnetic field strength and current and can be calculated with the following formula.

$$V = \frac{IB}{nde} \tag{21}$$

V is the voltage created, B stands for the strength of the magnetic field perpendicular to the conductor, I is the current, n the charge density, e the electron charge and d is the thickness of the conductor.
When measuring magnetic fields in open spaces, a flat probe is used which is the best one for measuring transverse magnetic fields. Via the probe a test current is send through the conductor, resulting in a voltage, which the meter records (23). When using one coil it can be assumed that the strongest field will be in the center of the coil, getting weaker when moving away from the loop. However, when two coils are used like in the Helmholtz Coils, the field will be strongest in the center, between the two coils, because it is the sum of both magnetic fields which are uniform throughout as can be seen in figure 9. During the one panel experiments a 03A Hall probe was used to measure the magnetic field strength in directions Bx, By and Bz for 3 different situations. The maximal magnetic field strength that PacMag should be able to produce is 50 mT. However it is possible that in practice this number can not be reached. To make sure that the SMP, which is centered between the two outer coils, will be placed under the desired magnetic field during testing, a few measurements need to be done. First, the Hall probe is placed at the central position with a magnetic field strength of 50 mT in the x-direction. In Appendix 7.1 the reference Cartesian coordinate system of the probe head is portrayed in comparison with the magnetic field orientation of PacMag. After reading out the maximally measured magnetic field strength with the probe, a new set of tests is done at that measured field. Lowering the magnetic field strength every time to the given Gauss meter value. This is to see if any deviations occurs between the script and the actual measured field. This procedure is repeated for the z-direction.

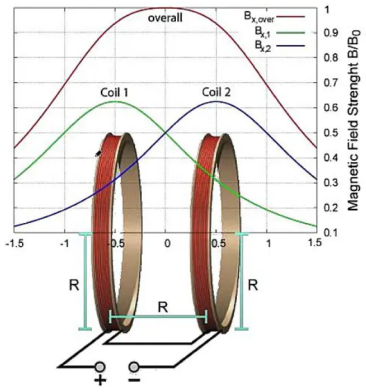

Figure 9: Magnetic field surrounding a pair of Helmholtz coils. Bx,over indicates the magnetic field sum of coil 1 and coil 2 which is higher than both maximal individual fields due to that the field runs uniformly throughout these coils (24).

3.1.2 Results Gauss Meter Experiments

From multiple measurements, when the magnetic field strength is set at 50 mT in the x-direction and z-direction, it can be concluded that the Gauss meter has a deviation of 2 mT compared to the set magnetic field strength in the code. The maximal field in the x-direction that was recorded is 41-42 mT, which is equal to 43-44mT in the PacMag script. However the z-plane can reach a higher magnetic field strength of 48 mT which is equal to the specified 50mT. For this reason further experiments do not exceed the limit of 45 mT in both directions.

3.2 Materials and Fabrication

The fabrication of the SMP samples and setup are immutable for both experiments, and will be explained in the following section.

3.2.1 SMP Samples

The SMP samples are made following a previously composed procedure, which can be found in Appendix 7.2. However, the molds and technique to making the SMP were varied to find the best result. SMP is made of two different materials, hardener and resin. To form a functional MP-3510 SMP sheet, these two have to be mixed in equal amounts. During this procedure it is important to minimize contact with air because this can lead to the formation of air bubbles, affecting the properties of the SMP. For this reason, a new device was tested which has two separate chambers and a mixer at the end, purposely mixing equal amounts of both materials without letting it come into contact with air. Once the mixture is poured into the mold, after conducting the steps described in Appendix 7.2, it is necessary to vacuum everything once again before curing it in the oven. This is to prevent any additional air bubbles from forming as would be the case if it were exposed to air in an open mold. The mold determines the shape and size of the panels by laser cutting the dimensions in one of the two plexiglass plates. Between these two plexiglass plates, a silicone sheet is placed to prevent the SMP from sticking to the bottom plate. The molds that were used for each of the experiments can be seen in figure 10.

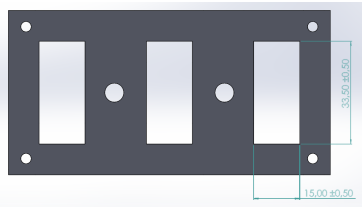

(a) Two panel mold in which 3 samples with dimensions 33,5x15x2mm SMP can be made.

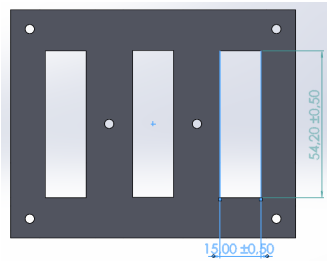

(b) Three panel mold in which 3 samples with dimensions 54.2x15x2mm SMP can be made.

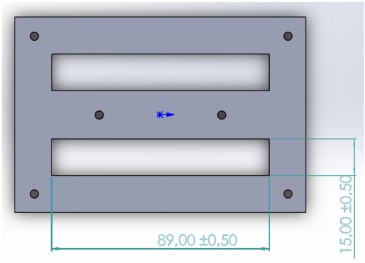

(c) Five panel mold in which 2 samples with dimensions 89x15x2mm SMP can be made.

Figure 10: (a) shows the two panel mold, (b) the three panel mold and (c) the five panel mold. Each can make multiple samples and the hinges are not incorporated into the design.

The hinges could not be incorporated in the design of the mold, and are therefore grafted by a laser cutter to the right dimensions. By adjusting the power and number of laser cut cycles a hinge with a height of 0.7mm, width of 15mm and 2.5mm length is made in each of the samples. The power was set to a value of 40 the speed to 30 and number of cycles to 9. In Appendix 7.3 all the combinations for power, speed and cycles are given. In figure 11 an example is given of an five panelled SMP sample with grafted hinges which was used during the four panel experiments.

Figure 11: A five panel SMP with laser cut hinges.

Once the SMP samples are produced, a permanent magnet made out of NdFeB is glued upon the sample using an instant adhesive superglue (Loctite 401). Three kinds of magnets are used throughout the experiments along with different orientations. The magnet orientations that are used in each experiment can be found in figure 12.

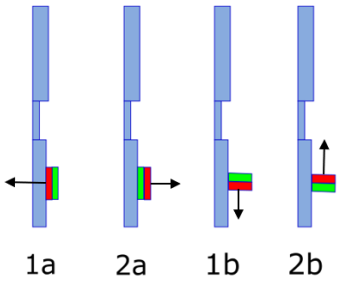

Figure 12: Red indicates the north-pole and green the south-pole, the arrow indicates the dipole moment vector. Magnets a are oriented in the horizontal direction and magnets b in the vertical direction. Only magnets expressed with number 1 will be used during the one panel experiments while the rest will be used in the remainder of the experiments.

3.2.2 Setup

The setup is immutable throughout the experiments and can be seen in figure 13.

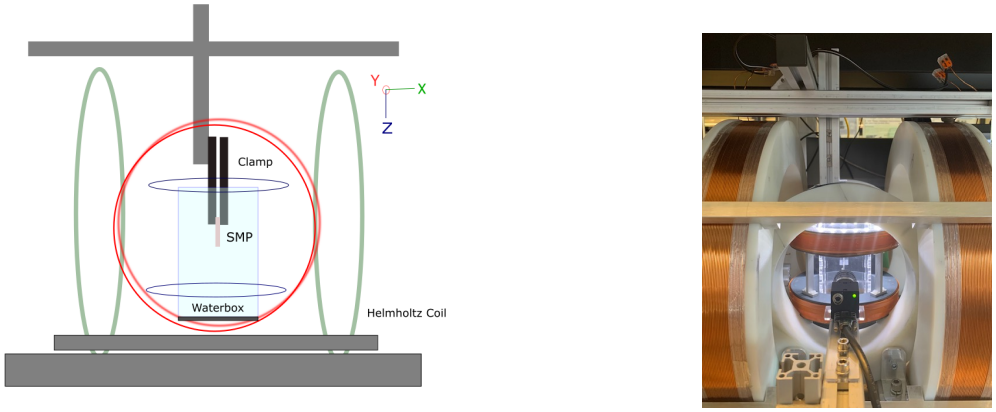

(a) Sketch of the setup.

(b) The actual setup.

Figure 13: In (a) a sketch of the used setup is given where the camera is assumed to be placed right in front of the SMP, recording its behavior when current is running through the outer Helmholtz coils and the material is heated beyond its glass transition temperature within the waterbox. In (b) the actual setup is displayed.

The setup consists of a couple of elements. Firstly, the SMP sample is secured at a structure hanging from the top bar in the vertical direction, with the magnetic moment aligned in the direction of the magnetic field. In the case of the Helmholtz coils this is in the x-direction. The sliding elements in this bar can purposefully be used to change the height from which the SMP hangs. This results in the fact that the same setup can be used for a two panel SMP sample as well as a five panel SMP sample, by securing it on an elevated height. To fix the SMP material, the outer panel is clamped between two plexiglass plates, as seen in Appendix 7.4 .

It is essential that the SMP material is completely submerged in water which is kept above the glass transition temperature of 37 degrees Celsius. This ensures that the SMP material is in its flexible state and can be influenced by magnetic actuation. To measure if this is the case, a MS6501 thermometer is used to measure the water temperature every few minutes. The waterbox is made out of 4mm plexiglas and has an outer dimensions of 75x75x140mm. Like above, the waterbox can be seen in Appendix 7.4. Last but not least, to be able to record experimental results a camera is secured in front of the setup, directly aligned with the SMP material.

4 Experiments

In this section the methodology and results for multiple conducted experiments will be presented. These include i) the one panel experiment, ii) the two panel experiments and iii) the four panel experiments. The one paneled experiments investigate the influence of temperature, magnetic field strength and orientation on two types of magnets with dipoles oriented in different directions. The two paneled experiments look into the possibility of making a V shape by testing different magnetic dipole ratios and field directions. The four paneled experiments consist of two rounds of testing, ultimately trying to realize one final shape, the zigzag.

4.1 One Panel Experiments

To measure the influence of magnetic actuation on the deformation of the SMP samples, there are several aspects that can be investigated. First of all, the temperature of water which leads to the flexible state of the SMP material. Secondly, the strength of the magnetic field. And lastly, the orientation of the magnetic field on the permanent magnet. In this section only the influence of magnet field strength and orientation will be described while the temperature tests can be found in Appendix 7.5. This first round of testing will be done with one magnet to eliminate any other influences like internal interactions.

4.1.1 Methodology Experiments

Magnetic Field Strength Considering that making a smart drug delivery system is the end purpose for this research, the magnet needs to be small enough not to influence the capability of transitioning into a miniaturized structure and at the same time be strong enough to be manipulated by magnetic actuation outside of the body. Because the magnet can be oriented two ways, with the dipole facing in the horizontal (a) or the vertical direction (b), two different magnets are used in a way that they will stay correlated. For the experiments with the magnet dipole facing in the horizontal direction one block magnet with dimensions 7x6x1.2mm is used with magnetizing strength of N50. To have almost equal magnetic strength in the vertical dipole orientation 7 magnets with dimensions 5x1.5x1mm and magnetization N45 are used. Presuming that the smaller magnets have more coating covering their surface the volume of magnetic material within diminishes, leading to the same magnetic strength that the 7x6x1.2mm magnet has also considering the difference in magnetizing strength. All these magnets with corresponding dipole moments are displayed in table 1. By applying multiple magnetic fields it is possible to test the influence of magnetic strength on the over-bending of the SMP material.

Table 1: *Table containing each magnet used with their corresponding dipole moment calculated with their magnetizing strength and dimensions.*

Magnets	Number used	Outer dimension (mm)	Magnetizing strength	Dipole moment (Am^2)
5x2x2	2	5x2x4	N45	42.81×10^{-3}
7x6x1.2	1	7x6x1.2	N50	57.35×10^{-3}
5x1.5x1	7	5x1.5x7	N45	56.19×10^{-3}

To determine the starting point, endpoint and the step size in magnetic field strength for this research multiple calculations are required. By rewriting and filling in formula 8 for a rotation of 30 degrees, the required magnetic field for a certain movement can be calculated as seen in formula 22 .

$$B = -K \cdot \frac{\pi}{6} \cdot \frac{1}{|\mu|} \cdot \frac{2}{\sqrt{3}} \tag{22}$$

The block magnet mentioned above with dimensions 7x6x1.2mm has a magnetic dipole moment of $57.35 \times 10^{-3}\ \mathrm{Am}^2$. And the seven combined block magnets with dimensions 5x1.5x1mm have a total

dimension of 5x1.5x7mm and therefor has a total magnetic dipole moment of about 56.19×10^{-3} Am^2. When filling in equation 7 for a hinge with a width of 15mm, height of 0.7mm and a length of 2.5mm the moment of inertia is about 1.372×10^{-3} kgm^4. Filling everything in gives that for a desired rotation of 30 degrees the required magnetic field is about 14.46 mT for the first case and 14.76 mT for the second as presented in table 2 . Both being around 15 mT. To be able to couple results to the theory, the starting magnetic field strength will be set at a starting value of 5 mT increasing it with that same value every time until reaching 45 mT, which should be equal to 90 degrees of rotation with steps of 10 degrees each time. The same is done in the negative field direction.

Table 2: *Table displaying all elements for calculating the magnetic field strength for each magnet used at a desired rotation of 30 degrees.*

Magnets	I,hinge (Kgm^2)	K,hinge (Pa)	μ (Am^2)	B (mT)
7x6x1.2	4.2875×10^{-13}	1.372×10^{-3}	57.35×10^{-3}	14.46
5x1.5x1	4.2875×10^{-13}	1.372×10^{-3}	56.19×10^{-3}	14.76

All these tests are run at the same temperature between 48 and 42 degrees Celsius because this range is far above the glass transition temperature that no change in plastic deformation is assumed and so that the water does not need to be replaced all the time. The orientation will stay constant in the x-direction, eliminating any other influences than the magnetic field strength self. The magnet is placed in the center of one of the panels with the south-pole facing outwards in the horizontal direction and upwards in the vertical plane always facing to the right like displayed in figure 12 as magnet 1a and 1b. All measurements will be recorded by the camera.

Orientation Field During these experiments the same procedure as in the magnetic field experiments is used as well as the same magnets and water temperature. The only variance is the magnetic field orientation. Rather than applying a magnetic field in the x-direction, a z-field is applied to investigate its influence on the different kinds of magnets.

4.1.2 Analysis

The recordings of the experiments will be analysed by measuring the end angle of the SMP, using an online protractor (25) as shown in figure 14. The end angle is assumed to be the angle the SMP takes on when it is in equilibrium and will therefore not change position anymore. In this case the torque created by the magnetic field will be equal to the force created within the SMP material due to the stiffness of the hinge. Multiple measurements have been done to average out any inaccuracies and keep the error as small as possible. The received data is analysed and plotted in the next chapter.

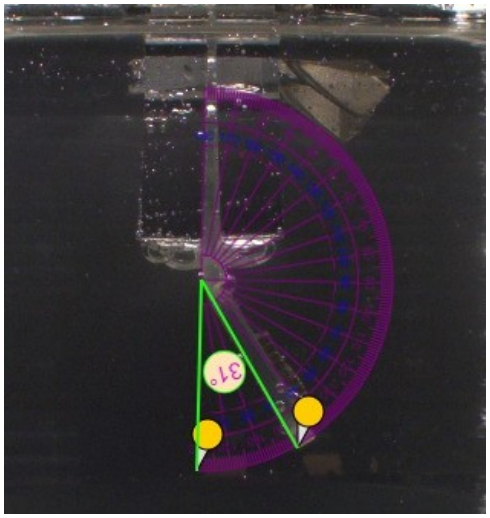

Figure 14: The angle indicated, is the maximal rotational angle when the SMP is in equilibrium and is therefore bend maximally.

4.1.3 Results One Panel Experiments

In figure 15 the results for two different magnets are displayed in the same graph. It portrays the influence of magnetic field strength when it is applied in the x-direction for two different magnet orientations. Magnet a has the magnet oriented in the same direction as the field, resulting in one way movement. In this case the SMP only shows movement in the positive axis at a starting point of about 20 to 25 mT. After it passes this threshold the rotational angle increases rapidly to an end value below 90 degrees rotation. Magnet b is oriented perpendicular to the magnetic field resulting in movement both at a negative and positive field. However the maximal rotation is much smaller than when the magnet has the same orientation as the field. The results can almost be mirrored at the center point of 0 mT. Examples of the results obtained at a constant magnetic field of +/- 40mT can be seen in figure 19.

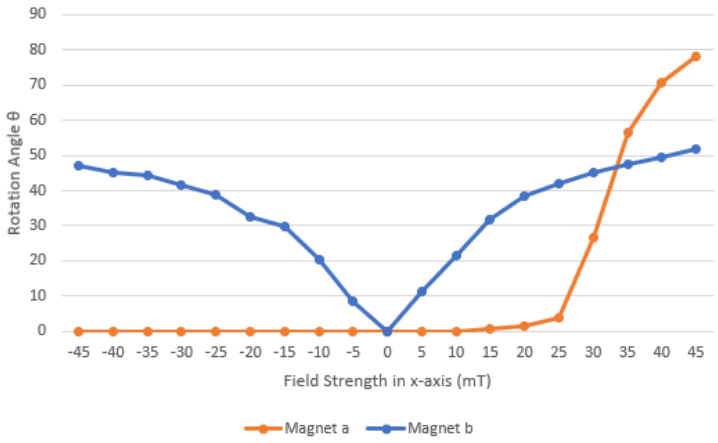

Figure 15: The figure portrays the Magnetic Field Strength Test. Each point indicates the maximal rotational angle of the SMP sample for two different magnets with a step size of 5 mT when the magnetic field is applied in the x-direction.

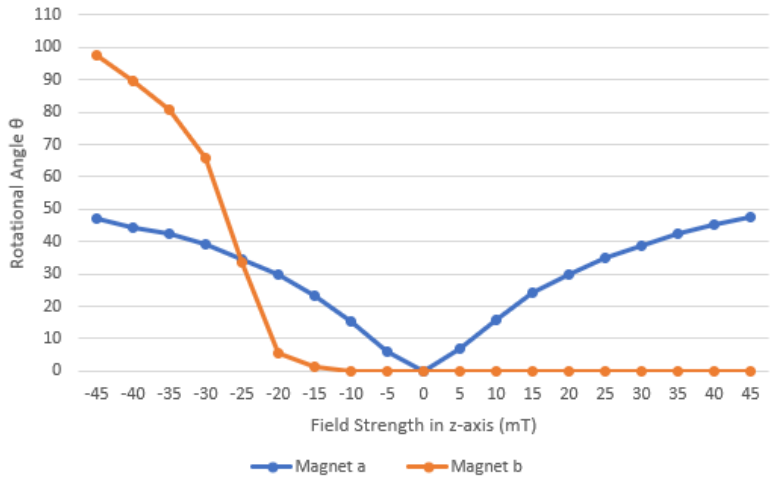

Figure 16: The figure portrays the Orientation Test. Each point indicates the maximal rotational angle of the SMP sample for two different magnets with a step size of 5 mT when the magnetic field is applied in the z-direction.

The orientation test in figure 16 shows almost the same results as the magnetic field strength except that the logarithmic curvature is now portrayed in the negative field and the maximal rotational angle surpasses 90 degrees. The threshold for magnet b, oriented parallel to the field is situated around -15 to -20 mT. So a lower magnetic field is necessary in the z axis compared to the x axis to exceed the threshold. Furthermore, magnet a which is situated perpendicularly is mirrored more perfectly than the magnetic field strength test but likewise stays below a rotational angle of 50 degrees. Examples of the results obtained at a constant magnetic field of +/- 40mT can be seen in figure 17.

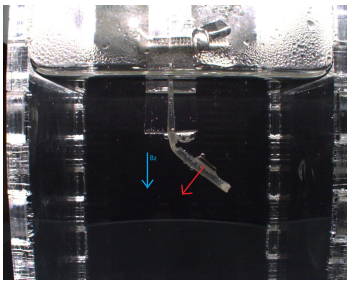

(a) Rotation of magnet 1a, perpendicular to the field, at 40mT.

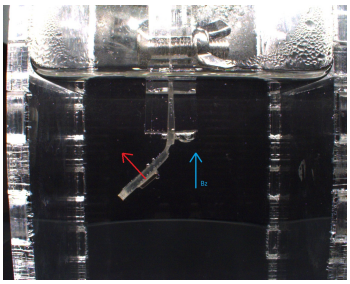

(b) Rotation of magnet 1a, perpendicular to the field, at -40mT.

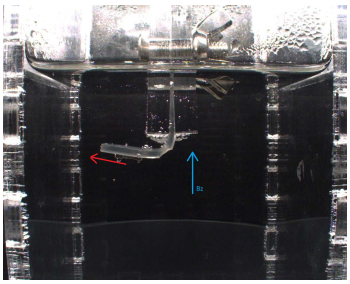

(c) Rotation of magnet 1b, parallel to the field, at -40mT

Figure 17: Rotation of magnets at a constant magnetic field strength in the z-direction. The red arrow indicates the direction of the magnetic moment vector and blue the direction of the magnetic field.

4.2 The Two Panel Experiments

In this section the results from the one panel experiments will be translated to a two panel case to see if it is possible to create a V shape. First, a geometrical analysis will be provided as well as an explanation to the approach of testing. Thereafter the results will be portrayed for multiple situations.

4.2.1 Background Information

From the one panel experiments it can be concluded that when a positive magnetic field in the x-direction is applied, magnet 1a which is now parallel to the magnetic field moves backwards (to the left). However, magnet 1b which is perpendicular to the field moves forward (to the right) when the field is positive. This way the directions in which the SMP moves, at one positive magnetic field strength, can alternate resulting in a zigzag shape when using multiple panels. These two movements at the same magnetic field strength are portrayed in subfigures 19a and 19b. However it was not taken into account during the one panel experiments that magnet a is in perfect misalignment with the magnetic field. This means that it can rotate 180 degrees both to the right as to the left to align its dipole moment vector with the external magnetic field. In this case it has a preferable rotation to the left, however when it is already misaligned to the right it is inclined to rotate that way. This is because the distance that needs to be covered to align with the external magnetic field when rotating farther to right is now smaller than to the left as portrayed in figure 18.

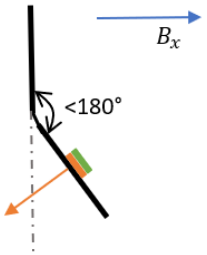

Figure 18: The angle the rotating panel makes on the right with the fixed panel is now smaller than to the left. This makes that the panel will rotate to the right instead of left. This is known as perfect misalignment.

However, perfect misalignment leads to unstable rotation. For this reason magnet 1b is flipped so that the north pole is facing upwards in the z-axis and the south pole is facing down like portayed in figure 12, which leads to a backwards rotation at the same magnetic field strength when applied in the x-direction, as can be concluded from figure 19c. This magnet is now called magnet 2b. Moreover, magnet a has a higher rotational angle at the same magnetic field strength as magnet b would have at that point when a field is applied in the x-axis. But this is only once a threshold of 20-25 mT is reached and the field stays positive. An explanation for this can also be the perfect misalignment. In that case, the dipole moment vector is oriented parallel to the external field and has a misalignment of 180 degrees instead of 90 degrees which leads to a greater tendency to rotate. The exact same conclusion can be made for opposite magnets when applying a z-field.

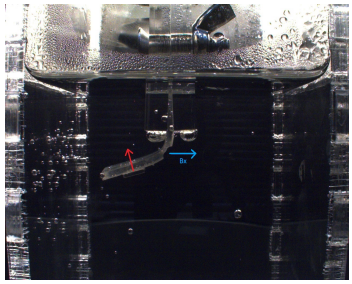

(a) Rotation of magnet 1a, parallel to the field, at 40mT.

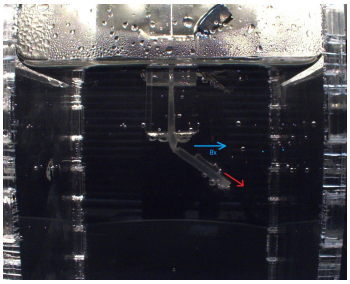

(b) Rotation of magnet 1b, perpendicular to the field, at 40mT.

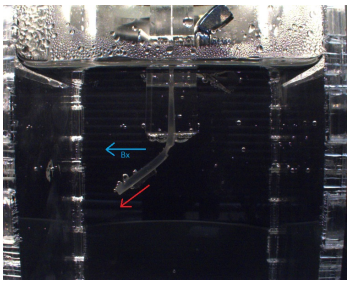

(c) Rotation of magnet 1b, perpendicular to the field, at -40mT

Figure 19: Rotation of magnets at a constant magnetic field strength in the x-direction. The red arrow indicates the direction of the magnetic moment vector and blue the direction of the magnetic field.

When creating a zigzag shape with 4 panels, since the top one is secured, the first hinge bends at a different angle than the rest. The first rotational angle is 45 degrees whereas all successive hinge rotational angles need to be 90 degrees as can be seen in figure 20. This also counts for a V shape made out of 2 panels. To calculate the amount of magnets that need to be used on each panel the two panel analysis described in chapter 2 was adopted.

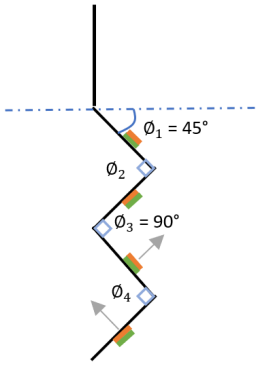

Figure 20: A four panel zigzag case where the top panel is secured in the vertical direction. The first rotational angle is equal to 45 degrees where after all the angles are equal to 90 degrees.

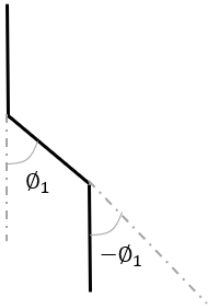

(a) Rotated z shape where ϕ_2 is equal to $-\phi_1$.

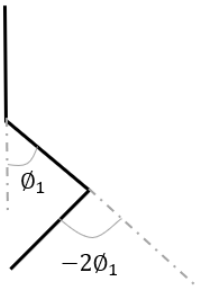

(b) V shape where ϕ_2 is equal to $-2\phi_1$.

Figure 21: The rotational angles of ϕ_2 denoted in a form of ϕ_1 depending on the shape the panels make.

In case that the structure makes a rotated z shape, like depicted in subfigure 21a, ϕ_2 is equal to $-\phi_1$. The ratio for magnet strength on panel 1 and 2 is then,

$$\frac{m_1}{m_2} = \frac{2}{cos(\phi_1)} \tag{23}$$

Filling in a rotational angle of 30 degrees for example, gives that the magnet on panel 1 needs to be about 2.5 times as strong as the magnet on panel two.

However, when creating a V shape out of the two panels, as can be seen in subfigure 21b, ϕ_2 is equal to $-2\phi_1$. This leads to an elimination of ϕ variables and a simplified ratio of,

$$\frac{m_1}{m_2} = \frac{3}{2} \tag{24}$$

In case magnets b are used, it is easy to alter the strength of the magnets, by simply attaching more or less block magnets to the panel. This way the dipole ratios for multiple panels can be varied using different magnet combinations.

4.2.2 Testing

It is desirable to limit the amount of magnets on each panel for end purposes. However, it is questionable if magnet b is strong enough when trying to meet the ratio of three over two when creating a V shape whilst limiting the number of magnets. For testing purposes both magnets a in the z-field direction will be tested as well as magnets b in the x-field direction. This should give similar results when they are of equal strength as can be concluded from the one panel experiments. However, because magnet a can not be defined by a ratio of three over two all ratios will become two over one.

Testing magnet a

Since magnet a is a bigger and stronger compared to magnet b, only two combinations with maximally two magnets on one panel are tested. Before the first round of testing, one magnet was placed on the distal panel to observe strength of this one magnet and the required external magnetic field for a desired rotation of at least 30 degrees. All other combinations that are tested can be found in table 3 with their predicted behavior. A summary of the rotational direction for each magnet orientation when subjected to a negative or positive field in the z-direction is depicted in figure 22. The direction of the magnetic dipole is alternated by placing magnet 1a on panel 1 and magnet 2a on panel 2. All tests are done by increasing the magnetic field strength in steps of 5mT in both the positive and the negative field. Hereby all measurements will be recorded by the camera.

Table 3: *Table displaying all combinations tested for magnet a and their predicted shape. Each column denoted with a panel number indicates the amount of magnets placed on that panel. The magnets get alternated in dipole direction starting with magnet 1a. The tail shape is when one panel is aligned vertically while one panel bends.*

Combination	Magnets panel 1	Magnets panel 2	Ratio	Shape
1	1	1	1:1	Tail
2	2	1	2:1	V shape

Magnet	Orientation	Rotational direction		Threshold
		+ mT	-mT	
1a	N/S	→	←	NO
2a	S/N	←	→	NO
1b	$\frac{S}{N}$	✖	←	-20 to -25 mT

Figure 22: A summary of the rotational direction for each magnet orientation when subjected to a negative or positive field in the z-direction.

Testing magnet b

The first step, when testing magnet b, is to find out what the minimal number of magnets is at which still a noticeable rotation can be achieved. When using two magnets on the distal panel, a noticeable rotation of about 30 degrees was achieved and therefore chosen to be the minimal number of magnets used. Four combinations are tested which can be found in table 4 with their predicted behaviour. A summary of the rotational direction for each magnet orientation when subjected to a negative or positive field in the x-direction is depicted in figure 23. The direction of the magnetic dipole is alternated by placing magnet 1b on panel 1 and magnet 2b on panel 2. All tests are done by increasing the magnetic field strength in steps of 5mT in both the positive and the negative field. Hereby all measurements will be recorded by the camera.

Table 4: *Table displaying all combinations tested for magnet b and their predicted shape. Each column denoted with a panel number indicates the amount of magnets placed on that panel. The magnets get alternated in dipole direction starting with magnet 1b. The tail shape is when one panel is aligned vertically while one panel bends. A line can be oriented either to the left or to the right.*

Combination	Magnets panel 1	Magnets panel 2	Ratio	Shape
1	2	2	1:1	Tail
2	2	4	1:2	Line
3	4	2	2:1	V shape
4	4	4	1:1	Tail

Magnet	Orientation	Rotational direction		Threshold
		+ mT	-mT	
1a	N/S	←	✖	20 to 25 mT
1b	$\frac{S}{N}$	→	←	NO
2b	$\frac{N}{S}$	←	→	NO

Figure 23: A summary of the rotational direction for each magnet orientation when subjected to a negative or positive field in the x-direction.

4.2.3 Results Two Panel Experiments

The results are split up in the two rounds of testing that were done, magnet a and magnet b. For each result a small analysis will be given.

Testing magnet a

The results will only be portrayed in the negative field direction for magnet a, considering that the panels move in the same manner both ways. The negative field however can results in a bit more bending due to the fact that the hinge is oriented on this side. In Appendix 7.6.1 an example of this behavior can be seen.

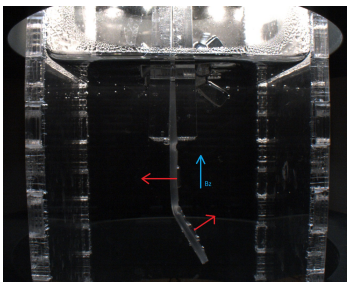

(a) Rotation of combination 1 at -15mT.

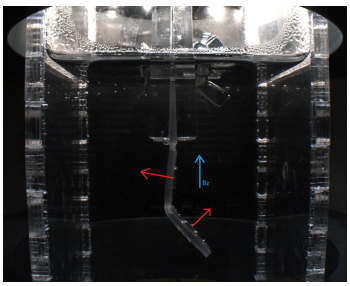

(b) Rotation of combination 1 at -30mT.

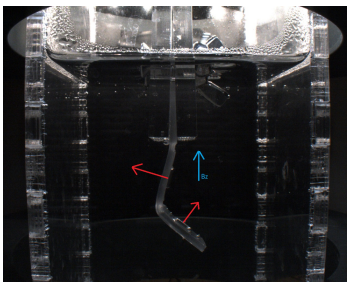

(c) Rotation of combination 1 at -45mT

Figure 24: Rotation of magnets at a constant magnetic field strength in the z-direction and a dipole ratio of 1:1. The red arrow indicates the direction of the magnetic moment vector and blue the direction of the magnetic field.

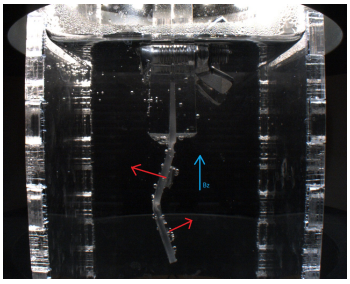

(a) Rotation of combination 2 at -15mT.

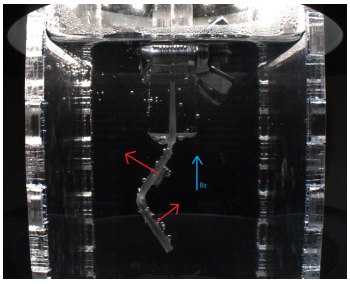

(b) Rotation of combination 2 at -30mT.

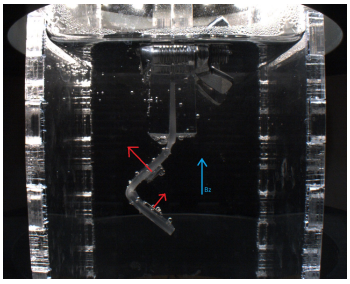

(c) Rotation of combination 2 at -45mT

Figure 25: Rotation of magnets at a constant magnetic field strength in the z-direction and a dipole ratio of 2:1. The red arrow indicates the direction of the magnetic moment vector and blue the direction of the magnetic field.

Both combinations that were tested for magnet a result in V shapes, as illustrated in figures 24 and 25. However like expected, a ratio of 2:1 is further inclined to create a V shape than a ratio of 1:1. However, ratio 1:1 does not result in a tail shape like expected due to misalignment. When the distal panel rotates with a sufficient angle that the proximal panel also rotates, the magnetic dipole moment is automatically misaligned leading to the rotation of the proximal panel. Furthermore, an increasing external magnetic field strength leads to a higher rotational angle for both cases.

Testing magnet b

Due to the fact that magnet b is not as strong as magnet a the results are not as clear. For this reason only the results in the positive field direction are depicted in figure 26 , which are more distinctive. In Appendix 7.6.1 the results in the negative field direction are given.

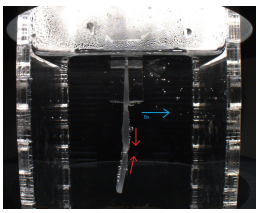

(a) Rotation of combination 1 at 45mT.

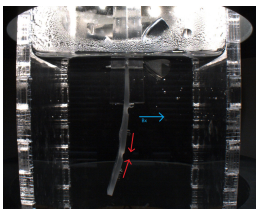

(b) Rotation of combination 2 at 45mT.

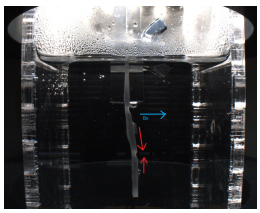

(c) Rotation of combination 3 at 45mT.

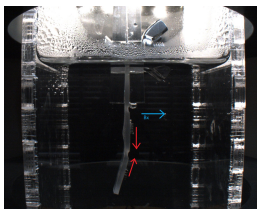

(d) Rotation of combination 4 at 45mT.

Figure 26: Rotation of magnets at a constant magnetic field strength in the x-direction. The red arrow indicates the direction of the magnetic moment vector and blue the direction of the magnetic field.

From the results in figure 26, it can be concluded that only slight rotations are possible even at the maximal magnetic field strength of 45 mT. This is probably because the magnetic dipole moment of these magnets are not sufficient. The magnetic dipole moment of a single magnet a is equal to the magnetic dipole moment of seven magnet b's. Therefore if only two magnet b's are used, then this dipole moment would only reach 2/7 of the dipole moment that magnet a has. Considering that in the second combination of testing with magnet a, two magnets were placed on one panel this would mean that fourteen magnet b's would be needed to create the same magnetic dipole moment. However the maximally used number of magnets is four.

4.3 The Four Panel Experiment

In this section the results from the two panel case will be elaborated to see if it is possible to create a third configuration, the zigzag shape. Starting off, only combinations with magnet 1a and 2a and a field in the z-direction will be made since these had the best results in the last section. Thereafter also tests will be run with the magnetic field in the x-direction. In this case a combination of magnets 1a, 1b and 2b will be used. However, the analysis will be split up in vertical magnet placement and horizontal placement.

4.3.1 Testing

Testing Magnet a

In this section, the two panel experiments for magnet a will be expanded towards four panel experiments to see if it is possible to create a zigzag shape. Again, multiple combinations are tested to see what the influence of each magnet on the implicated panel is. All these combinations can be found in table 5. It is expected that combination two and five will come closest to a zigzag shape. This is because the proximal panel needs to be stronger than the second panel due to calculations explained earlier. Also by alternating the strength of the magnetic dipole on each panel, it is expected that they are not inclined to cancel each other out and will therefor result in a zigzag shape. The maximum number of magnets used is two per panel, and the dipole direction is alternated like in the two panel experiments starting with magnet 1a. All tests are done by increasing the magnetic field strength in steps of 5mT in both the positive and the negative field until a maximum of +/- 45mT. Hereby all measurements will be recorded by the camera.

Table 5: *Table displaying all combinations tested for magnet a. Alternating between 1a and 2a. Each column denoted with a panel number indicates the amount of magnets placed on that panel.*

Combination	Panel 1	Panel 2	Panel 3	Panel 4
1	1	1	1	1
2	2	1	1	1
3	2	2	1	1
4	2	2	2	1
5	2	1	2	1

Testing Other Combinations

Multiple tests are executed to find the optimal combination of magnet placement when using magnets 1a, 1b and 2b. The first step is to create a V shape with two panels (like in the previous section) or with the entire four paneled structure. After analyzing the interaction between magnets and the magnetic field an attempt will be made to create the zigzag shape.

To first create a V shape multiple tests are done by attaching magnets on only two panels. Multiple combination of attaching magnets on panels 1 and 3, 2 and 4 or 1 and 2 are made, disregarding the first fixed panel. When using magnet a, a threshold needs to be passed before any movement occurs, leading to a decrease in the possible number of magnet b's that can be used and a obligatory higher magnetic field strength. However when rotating magnet 1b so that the north-pole is facing upwards and south-pole downwards (defined as magnet 2b) the magnetic field strength can be set at a lower value whilst still achieving a rotational angle in the negative direction like magnet 1a. A combination of magnet 1a and 1b or 1b and 2b are used in the first set of experiments with the two panel V shape. These combinations can be found in table 6.

Table 6: *Table displaying all combinations in the first round of testing to create a V shape. The number in () indicates the number of magnets used.*

Combination	Panel 1	Panel 2	Panel 3	Panel 4
1	-	Magnet 1b (6)	-	Magnet 1a (1)
2	-	Magnet 1b (3)	-	Magnet 2b (3)
3	-	Magnet 1b (6)	-	Magnet 2b (3)
4	Magnet 1b (3)	Magnet 1a (1)	-	-
5	Magnet 1b (3)	Magnet 2b (3)	-	-
6	Magnet 1b (5)	Magnet 2b (3)	-	-
7	Magnet 1b (2)	Magnet 2b (2)	-	-
8	Magnet 1b (2)	-	-	Magnet 2b (2)
9	Magnet 1b (2)	Magnet2b (2)	Magnet 1a (1)	-

After the first round of testing, magnets are placed on all four panels to further investigate their influence and explore if there is a possibility to create the zigzag shape. The combinations tested can be found in table 7.

Table 7: *Table displaying all combinations in the second round of testing to create a zigzag shape. The number in () indicates the number of magnets used.*

Combination	Panel 1	Panel 2	Panel 3	Panel 4
10	Magnet 1b (6)	Magnet 2b (3)	Magnet 2b (3)	Magnet 1b (3)
11	Magnet 1b (6)	Magnet 2b (3)	Magnet 2b (5)	Magnet 1b (3)
12	Magnet 1b (6)	Magnet 2b (3)	Magnet 1a (1)	Magnet 1b (3)
13	Magnet 1b (6)	Magnet 1b (3)	Magnet 2b (3)	Magnet 1a (1)
14	Magnet 1b (6)	Magnet 1b (3)	Magnet 2b (3)	Magnet 2b (6)
15	Magnet 1b (2)	Magnet 1b (3)	Magnet 2b (3)	Magnet 2b (2)
16	Magnet 1b (2)	Magnet 1b (1)	Magnet 2b (1)	Magnet 2b (2)
17	Magnet 1b (3)	Magnet 2b (2)	Magnet 1b (3)	Magnet 2b (2)
18	Magnet 1b (2)	Magnet 2b (2)	Magnet 1b (2)	Magnet 2b (2)

4.3.2 Results Four Panel Experiment

Testing Magnet a

In figure 27 the results for all the combinations tested with magnet a are depicted. All results are only given for the negative field like in the two panel experiments. In Appendix 7.6.2 the results in the positive field can be found.

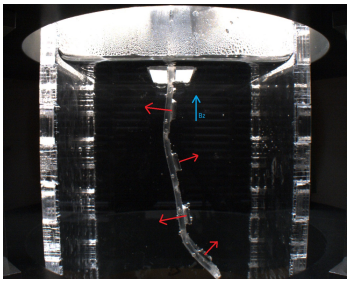

(a) Zigzag for combination 1.

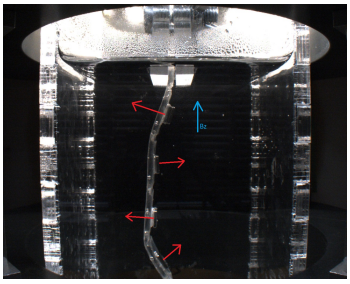

(b) Zigzag for combination 2.

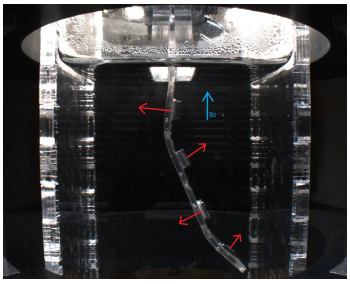

(c) Zigzag for combination 3.

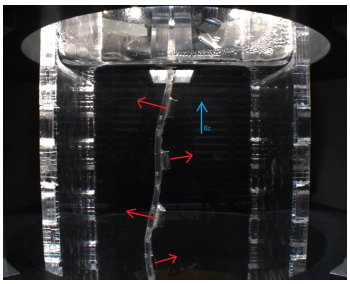

(d) Zigzag for combination 4.

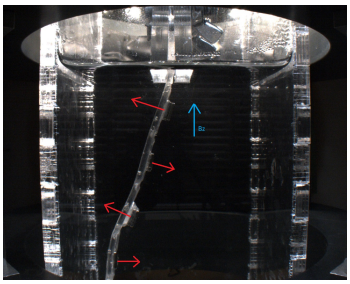

(e) Zigzag for combination 5.

Figure 27: Rotation of magnets on all panels at a constant magnetic field strength in the negative z-direction. The red arrow indicates the direction of the magnetic moment vector and blue the direction of the magnetic field.

As displayed in figures 27a to 27e are the results very different than would be expected from the two panel results. The prediction that combination 2 and 5 would give the best results are thereby refuted. In this case combination 4 has most similarities with a zigzag shape, although it is more portrayed as a curvature. The proximal panel is in this case is two times as strong as the distal panel, like calculated. However the middle two panels also need to have two magnets to overcome the internal interactions of the dipole moment vectors.

Testing Other Combinations

From previous results it can be concluded that the panels move in different directions when subjected to the same magnetic field depending on the magnet orientations, as already described in subsection 4.2.1. In figure 28 a clear overview of the expected behavior for each magnet from the one panel experiments, at a positive or negative magnetic field strength is portrayed.

Magnet	Orientation	Rotational direction		Threshold
		+ mT	-mT	
1a	N/S	←	✖	20 to 25 mT
1b	$\frac{S}{N}$	→	←	NO
2b	$\frac{N}{S}$	←	→	NO

Figure 28: A summary of the rotational direction for each magnet orientation when subjected to a negative or positive field. The colors of the magnet number correspond to the colored dots in the drawings.

The optimal combination to create a zigzag shape has not been found although this was expected from theory and previous observations. This is most likely due to internal interactions between the magnets, although this is not visible when no external magnetic field is applied. Moreover, there are some situations within a 4 panel structure like dipole misalignment due to rotation which could

not be foreseen during the one panel experiments. Nevertheless, there are some clear observations that can be made for each of the magnets. In the following sections a distinction will be made between the magnets with a horizontal dipole direction (a) and a vertical dipole direction (b). First, the behavior of magnet 1b and 2b will be observed and substantiated where after the behavior of magnet a will be examined.

Vertical Magnet Placement:

In figure 29 an overview of the panel movement at key sequences noted in tables 6 and 7 for magnet combination 1b and 2b can be found[2]. These sketches are made to be able to draw clear conclusions for the behavior of the magnet. In figure 30 the actual results are given.

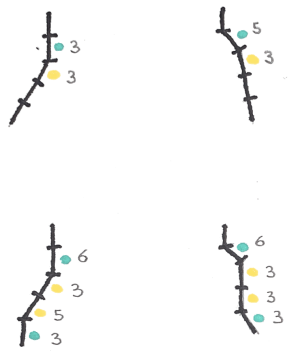

Figure 29: Key observations for magnet 1b and 2b when subjected to a positive field, using two magnets or four magnets. The colors indicate which magnet is attached on each panel. Clockwise, the combinations portrayed are 5, 6, 8 and 9.

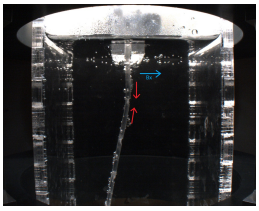

(a) Zigzag for combination 5.

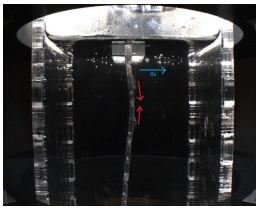

(b) Zigzag for combination 6.

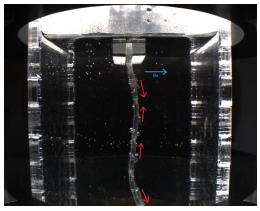

(c) Zigzag for combination 8.

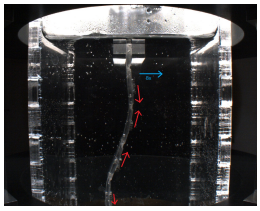

(d) Zigzag for combination 9.

Figure 30: Rotation of magnets on all panels at a constant magnetic field strength in the positive x-direction. The red arrow indicates the direction of the magnetic moment vector and blue the direction of the magnetic field.

As can be seen in the top two sketches both magnet 1b and 2b move in the foreseen direction, yellow to the left and blue to the right at a positive field. Furthermore, when one magnet is stronger, due to the placement of more magnets on one panel compared to the other, this rotational direction is dominant. However, it does seem that when they are equal in strength the magnet on the distal panel has the overhand. Another observation made from the bottom sketches, is that when rotation occurs in one direction an antagonistic magnet first needs to align the panel in a perpendicular state before rotation in the other direction can occur. Rotation in this case is only possible when a stronger magnet is used, as can be seen in the bottom left sketch. All these points mentioned above seem to correlate with the results of the one panel experiments, but there is one exception.

[2]Key sequences are the combination of magnets for which the SMP-structure rotates in such a way that a coherent explanation can be given on the behavior of the magnet.

The rotational angle does not seem to be as large as would be expected.

Horizontal Magnet Placement:

In figure 31 an overview of the panel movement at key sequences noted in tables 6 and 7 for magnet 1a and 2a can be found. These sketches are made to be able to draw clear conclusions for the behavior of the magnet. In figure 32 the actual results are given.

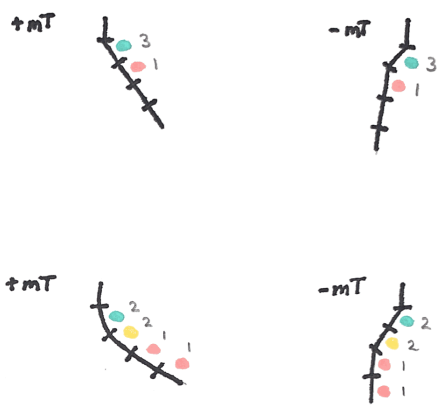

Figure 31: Key observations for magnet a using two magnets and using four magnets. The colors indicate which magnet is attached on each panel. The top two sketches are combination 4 in the positive and the negative field. And the bottom two are combinations 11.

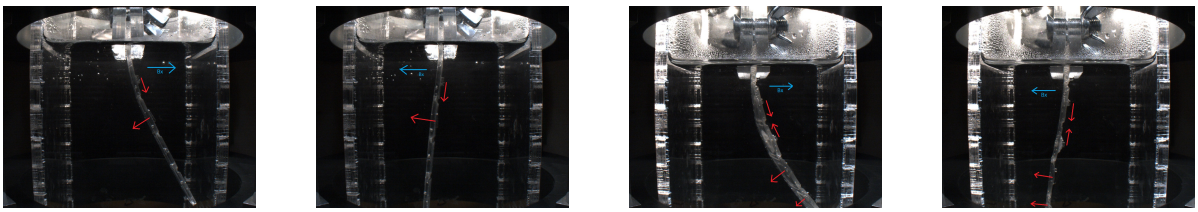

(a) Zigzag for combination 4 with a positive field direction.

(b) Zigzag for combination 4 with a negative field direction.

(c) Zigzag for combination 11 with a positive field direction.

(d) Zigzag for combination 11 with a negative field direction.

Figure 32: Rotation of magnets on all panels at a constant magnetic field strength in the x-direction. The red arrow indicates the direction of the magnetic moment vector and blue the direction of the magnetic field.

Magnet a does not seem to play a role in the experiments as expected. Even when the magnetic field strength surpasses the threshold of 20-25 mT no movement to the left seems to occur, like in the top left sketch. Only when applying the magnetic field in the negative direction, magnet a is inclined to move forward like portrayed in the top right sketch. This goes against the theory and observations during preliminary testing. However, in the one panel experiments it was not taken into account that when a magnet is oriented parallel to the field, it is perfectly misaligned. So, the rotation is 180 degrees in each direction. Due to misalignment, magnet a can now not only move to the left at a positive field but also to the right when it is already oriented in this direction. This causes for very unstable rotation and results like can be seen in the bottom of figure 31.

5 Discussion

This discussion is split up in four subsections. These include i) SMP and Setup, ii) the one panel experiment, iii) the two panel experiments and iv) the four panel experiments.

5.1 SMP and Setup

As mentioned earlier, there was no accessible procedure for making clean sheets of SMP. Therefore multiple elements were adjusted and tested. One obstacle that was encountered was that the SMP would stick to the mold. However, anti-stick spray led to the formation of more air bubbles. For this reason, only a silicone sheet was used between the two plexiglass plates. Nevertheless this resulted in that the SMP would still stick to the sides of the mold. To be able to get the SMP out, the mold had be broken and the SMP would need to be cut from the edges, leading to impurities. Also excess SMP that flowed over the mold was cut from the sides which might influence the characteristics of the material. Additionally, batches needed to be made in abundance because of the new two chamber pistol. In case insufficient amounts of Resin A and Hardener B were poured into the chambers, the mixer did not work properly and would only produced more air bubbles. Next, it is essential that Resin A and Hardener B are mixed in equal amounts, whenever this was not the case the SMP would not set in the oven. Therefore the first and the last bit of the mixture were not poured into the mold to prevent this from happening. Even though the steps to making SMP did not differ, the batches would still be unique. This leads to deviations in results. What also led to deviations in possible rotational angels, were the hinges. The hinges were lasercut because they could not be incorporated into the design of the mold. Even though the same settings were used on each SMP sheet it seemed that the dimensions of the hinges differed over the various batches of SMP. This was mainly due to the fact that the sheets were not always completely flat, because of the placement of the silicon sheet. Bumps in the sheet lead to variance in sheet-laser distance and therefore hinge dimensions. Furthermore, when laser-cutting, the laser has to be placed in the exact same manner to get the hinge at corresponding distances from each other. However this was done manually and can therefore not be perfect. Like in any other research, multiple steps were done manually like securing the panel between the two plexiglass plates at a certain height in the setup or placing the magnets on the panels. All these variables can be assumed as imperfect and therefore as not constant.

5.2 One Panel Experiments

The water temperature in all the conducted tests during the one, two and four-panel experiments was situated around 42 to 48 degrees. This range was chosen because it is situated far above the glass transition temperature and no change in elastic state was assumed. However, it seemed that rotation became harder after a few rounds of test because of the decreasing water temperature. Nevertheless, the procedure to testing was therefore not changed. To determine the starting point, step size and the end point of the magnetic field strength and orientation test, a few calculations were done. Within these calculations, the dimensions of the hinge were used. Like mentioned above, it cannot be validated that the hinge dimensions are constant for all SMP samples. Moreover, an estimation was made of the average dimensions. Therefore the magnetic field strength that would be needed for a rotation of 30 degrees can differ over the multiple SMP batches.

The analyses for the one panel experiments was done with an online protractor. The end angle that was measured, was assumed to be the angle the SMP takes on when it is in equilibrium and will therefore not change position anymore. However, the time it took for the SMP sample to be in equilibrium differed per experiment. Due to the fact that this was concluded by observation the results between sets of experiments could differ. Additionally, the end angle that was chosen as point on the protractor was done by eye and can therefore be imperfect. Last but not least, due to some inconclusive results for magnet b during the magnetic field strength test, these were redone

and tested more frequently than the rest.

The results from the one panel experiments can be explained by the term perfect misalignment. However this was discovered much later. The first test that was done for the one panel experiments was the temperature test, however this was moved to Appendix 7.5 because the results were inconclusive. As can be seen from the results is the outcome almost linear. However, it would be expected that there would be a steep slope around the glass transition temperature. This is because below the glass transition temperature the switching segments should lock and limit possible deformation. Nevertheless, what was not taken into account is that the elastic modulus changes for MP-3510 in a transition area between 20 and 60 degrees. And as can be seen in figure 39 only tests were done within this region. For this reason no conclusion can be drawn from this set of experiments.

5.3 Two Panel Experiments

The two panel experiments were conducted after no conclusion could be drawn from the four panel experiments with magnets 1a, 1b and 2b. It was not till then that the problem with perfect misalignment was found. For this reason one set of experiments was done to investigate the behavior of magnets in the horizontal direction (a) and separately for the behavior of magnets in the vertical direction (b). In the first attempts, tests were done with magnet a in case of perfect misalignment. But due to the fact that a SMP sample will never be perfectly straight still only one rotation was observed. Therefore the perspective on testing changed, and all experiments were conducted with the field perpendicular to the dipole moment vector. In table 3 it was predicted that only ratio 2:1 would lead to a V shape. However from the results it can be concluded even ratio 1:1 can lead to a V shape when the magnet is strong enough. An explanation for this can be that when the misalignment of the second panel increases the rotation around the hinge also increases. When this happens the proximal panel rotates a bit, leaving the state of perfect misalignment and leading to a torque. Even though the results for ratio 2:1 seem almost perfect for magnet a, the calculations do not completely support the results. The calculations indicate that at a ratio of 3:2 ϕ_2 is equal to $-2\phi_1$, leading to a perfect V shape. During the experiments however a ratio of 2:1 was used, yet for this ratio no analytical solution for ϕ_1 and ϕ_2 was found.

In case of magnet b, only slight rotations for a maximal field strength of 45mT were seen. As explained earlier, this was probably due to minimal magnetic dipole moment compared to magnet a. To indicate if this was true new tests should have been done with more magnets to confirm.

5.4 Four Panel Experiments

As mentioned in the previous section, tests with magnet combinations 1a, 1b and 2b for the four panel experiments were done before any other experiments. Another four panel test for magnets in the horizontal direction were added because improved results came from the two panel experiments with magnet a. There was only time to check the five combinations once for the magnet oriented in the horizontal direction (a) and the results are to be presumed as true from those observations. As mentioned in the results the final outcomes do not match the hypothesis. This can be explained by the influence of internal interactions, however there is no hard proof for this.

The experiments portrayed in figures 30 and 32 were conducted twice for analysis. However the results showed two different degrees of bending for the same experiment. This is probably because in the second set of experiment a new SMP sheet was used while for the first round of testing multiple experiments were already conducted with this sheet. It can be concluded that when the sheet is used regularly the dimensions of the hinge change and the stiffness of the hinge decreases. Therefore, the SMP sheets need to be renewed more often to limit this effect.

6 Conclusion and Future Work

The goal of this research was to investigate the influence of strength and orientation of magnetic actuation on a SMP-based origami structure to see if it was possible to create third configuration, the zigzag shape. During this study multiple steps were taken to reach this final goal. The results show that it is possible to deform the SMP-based origami structure beyond its permanent and temporary state into a V shape configuration when using magnets that are oriented perpendicular to the field and have a magnetic dipole moment with a minimal value of 57.35×10^3 Am^2. However it is harder to realize great rotations when using multiple panels. This is due to internal interactions. For future work perfect misalignment should be investigated as well as the amount of influence the magnetic dipole moment of a magnet has on the overall rotational angle in equilibrium.

Another point for future work is to see if it is possible to make the dimensions of the SMP structure smaller so that the magnetic strength needed can be limited. Moreover, it should be investigated if there is a cleaner way to make the hinges. This would lead to more uniform results and possible minimization of rotational stiffness. An option is to add the hinge to the bottom plate or even better, making a 3D mold with the hinge incorporated into the design.

References

[1] F. Leong, N. Garbin, C. D. Natali, A. Mohammadi, D. Thiruchelvam, O. Denny, and P. Valdastri, "Magnetic Surgical Instruments for Robotic Abdominal Surgery," *Reviews in Biomedical Engineering*, vol. 9, pp. 66–78, 2016. [Online]. Available: https://doi.org/10.1109/RBME.2016.2521818

[2] M. Tonutti, D. S. Elson, G. Z. Yang, A. W. Darzi, and M. H. Sodergren, "The role of technology in minimally invasive surgery: State of the art, recent developments and future directions," *Postgraduate Medical Journal*, vol. 93, no. 1097, pp. 159–167, 2017.

[3] H. Reza Rezaie, M. Esnaashary, A. Aref arjmand, and A. Öchsner, "The History of Drug Delivery Systems." Springer, Singapore, 2018, pp. 1–8. [Online]. Available: https://link.springer.com/chapter/10.1007/978-981-10-0503-9_1

[4] A. R. Ahmed, O. C. Gauntlett, and G. Camci-Unal, "Origami-Inspired Approaches for Biomedical Applications," *ACS Omega*, vol. 6, no. 1, p. 46, 1 2021. [Online]. Available: https://www.ncbi.nlm.nih.gov/pmc/articles/PMC7807481/

[5] M. Johnson, Y. Chen, S. Hovet, S. Xu, B. Wood, H. Ren, J. Tokuda, and Z. Tsz Ho Tse, "Fabricating biomedical origami: a state-of-the-art review," *International journal of computer assisted radiology and surgery*, vol. 12, no. 11, p. 2023, 11 2017. [Online]. Available: https://www.ncbi.nlm.nih.gov/pmc/articles/PMC5922460/

[6] S. Erkeçoglu, A. D. Sezer, and S. Bucak, "Smart Delivery Systems with Shape Memory and Self-Folding Polymers," in *Smart Drug Delivery System*. IntechOpen, 2 2016. [Online]. Available: undefined/state.item.id

[7] J. C. Griffis, "Design," in *Shape-Memory Polymer Device Design*. Elsevier, 1 2017, pp. 23–75.

[8] N. Ebrahimi, C. Bi, D. J. Cappelleri, G. Ciuti, A. T. Conn, D. Faivre, N. Habibi, A. Hošovský, V. Iacovacci, I. S. M Khalil, V. Magdanz, S. Misra, C. Pawashe, R. Rashidifar, P. Eduardo David Soto-Rodriguez, Z. Fekete, and A. Jafari, "Magnetic Actuation Methods in Bio/Soft Robotics," *Advanced Functional Materials*, vol. 31, no. 11, p. 2005137, 3 2021. [Online]. Available: https://onlinelibrary-wiley-com.ezproxy2.utwente.nl/doi/full/10.1002/adfm.202005137

[9] S. V. Cox, "Optimisation of origami structures for magnetic actuation in minimally invasive surgery," *BSc thesis, University of Twente*, 2022.

[10] E. Morsink, "Magnetic Actuation of Shape Memory Polymer-base Origami Structures," *BSc thesis, University of Twente*, 2022.

[11] M. Meloni, J. Cai, Q. Zhang, D. Sang-Hoon Lee, M. Li, R. Ma, T. Emilov Parashkevov, and J. Feng, "Engineering Origami: A Comprehensive Review of Recent Applications, Design Methods, and Tools," *Advanced Science*, vol. 8, no. 13, p. 2000636, 7 2021. [Online]. Available: https://onlinelibrary.wiley.com/doi/full/10.1002/advs.202000636

[12] M. Behl and A. Lendlein, "Shape-memory polymers," *Materials Today*, vol. 10, no. 4, pp. 20–28, 4 2007.

[13] D. L. Safranski, "Introduction to Shape-Memory Polymers," in *Shape-Memory Polymer Device Design*, 2017, pp. 1–22. [Online]. Available: http://dx.doi.org/10.1016/B978-0-323-37797-3.00001-4

[14] G. Baer, T. S. Wilson, D. L. Matthews, and D. J. Maitland, "Shape-memory behavior of thermally stimulated polyurethane for medical applications," *Journal of Applied Polymer Science*, vol. 103, no. 6, pp. 3882–3892, 3 2007. [Online]. Available: https://onlinelibrary.wiley.com/doi/full/10.1002/app.25567

[15] "Shape Memory Polymer SMP Technologies Inc.DiAPLEX." [Online]. Available: http://www2.smptechno.com/en/smp/

[16] B. Yang, W. M. Huang, C. Li, and L. Li, "Effects of moisture on the thermomechanical properties of a polyurethane shape memory polymer," *Polymer*, vol. 47, no. 4, pp. 1348–1356, 2006.

[17] Y. Kim and X. Zhao, "Magnetic Soft Materials and Robots," *Chemical Reviews*, vol. 122, no. 5, pp. 5317–5364, 2022.

[18] Z. Yang and L. Zhang, "Magnetic Actuation Systems for Miniature Robots: A Review," *Advanced Intelligent Systems*, vol. 2, no. 9, p. 2000082(1of18), 9 2020. [Online]. Available: https://onlinelibrary.wiley.com/doi/full/10.1002/aisy.202000082

[19] J. Hwang, J.-Y. Kim, and H. Choi, "A review of magnetic actuation systems and magnetically actuated guidewire- and catheter-based microrobots for vascular interventions," *Intelligent Service Robotics*, vol. 13, pp. 1–14, 2020. [Online]. Available: https://doi.org/10.1007/s11370-020-00311-0

[20] V. K. Venkiteswaran and S. Misra, "Towards gradient-based actuation of magnetic soft robots using a six-coil electromagnetic system," in *IEEE International Conference on Intelligent Robots and Systems*, 2020, pp. 8633–8639.

[21] T. L. Thomas, J. Sikorski, G. K. Ananthasuresh, V. K. Venkiteswaran, and S. Misra, "Design, Sensing, and Control of a Magnetic Compliant Continuum Manipulator," *IEEE Transactions on Medical Robotics and Bionics*, 2022. [Online]. Available: https://ieeexplore.ieee.org/stamp/stamp.jsp?tp=&arnumber=9878161

[22] "Helmholtz Coil." [Online]. Available: https://www.accelinstruments.com/Helmholtz-Coil/Helmholtz-Coil.html

[23] "What is a Gauss Meter? How does it work? - Metravi Instruments." [Online]. Available: https://www.metravi.com/what-is-a-gauss-meter-or-magnetometer/

[24] P. Ninja, "Magnetic Field from a Helmholtz Coil," 2020. [Online]. Available: https://www.youtube.com/watch?v=_6bKJrGCuJk&ab_channel=PhysicsNinja

[25] "Online Protractor — Angle Measuring Tool." [Online]. Available: https://www.ginifab.com/feeds/angle_measurement/

7 Appendix

7.1 Gauss Meter Probe

In figure 33 the Cartesian coordinates of the 03A probe can be seen and next to it is a sketch of the coordinate system within PacMag. This way the magnetic field strength running throughout the coils in each orientation can be coupled to the measurements given by the Gauss meter.

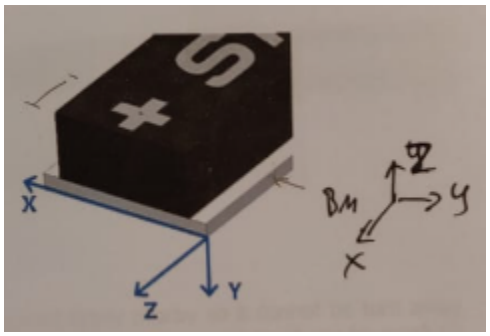

Figure 33: The orientation of a 03A Hall probe

7.2 SMP Procedure

As mentioned in Chapter 2.2 to create SMP two substances, resin A and hardener B, needed to be mixed according to a certain procedure. For this a manufacturers recipe found in figure 34 was edited to a new procedure which can be seen in figure 35.

(a) Preparation
- Dry liquid A and B for more than 1 hour at less than 50 Torr.
- Dry the die for more than 1 hour at 70 °C.

(b) Potting
- Place liquid A and B into vacuum chamber of less than 50 Torr.
- Mix liquid A and B, stirring for 30 sec. at 60 rpm.
- Immediately after stiring, pot the mixed solution to the die.
- After confirming that the solution flows into the die completely, discharge the vacuum.

(c) Curing and Removal
- Remove the die from vacuum chamber to the temperature and place into chamber.
- Cure the material for 1 – 2 hours at 70 °C
- Remove the finished product from the die.
- If necessary, cure an additional 1 – 2 hours at 70 °C.

Figure 34: Manufacturers recipe to SMP.

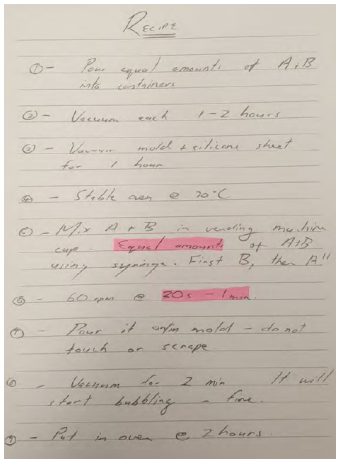

Figure 35: Elikes procedure to making SMP.

However when following these steps a lot of air bubbles arised diminishing the natural properties of SMP. To overcome this problem a pistol with two chambers and a mixer at the end was used instead of the cups. This lead to the possibility of mixing the two substances without letting them come into contact with air. This new device simplified the steps that needed to be taken for a clean sheet of SMP material. The steps that were taken are as follows:

1. Pour equal amounts of A + B into the two separate chambers
2. Close off chambers with transparent stoppers and place the chamber upside down in a cup with the gray cap screwed off
3. Vacuum for at least 1 hour
4. Place the mixer at the end and secure the two chambers in the pistol

5. Pour the mixture in the mold without using the first and last bit of the mixture
6. Vacuum for two minutes, it will start bubbling (do not touch even when it leaks from the sides)
7. Cure in oven for two hours

In figure 36 the course of the samples can be seen starting with the stirred sample till the last batch that was used throughout the experiments.

Figure 36: First SMP samples made, with the bottom one being mixed in two separate cups and the first one being a perfect sheet.

Multiple experiments were conducted testing different parameters. For example an anti-stick spray was used on the plexiglass plates in the hope the SMP would not stick to the sides of the mold anymore. However, a reaction occurred between the spray and the SMP material leading to more air bubbles. Also, vacuuming before curing in the oven appears to reduce air bubbles compared to skipping this step. And last but not least, the material is more likely to set when mixing in larger amounts.

7.3 Hinge Laser-cut Setting

The hinges could not be incorporated in the design of the mold and are therefore grafted by a laser cutter to the right dimensions. Multiple combinations were tried out to determine the correct power, speed and number of cycles that would be needed to cut the hinge to the right dimensions. In table 8 all combinations are given with a short description of their behavior.

Table 8: *Table displaying all combinations tested for making a hinge with dimensions 15x2.5x0.7mm.*

Combination	Power	Speed	cycles	Behavior
1	30	10	1	smooth but shallow
2	30	10	2	1/2 depth, melted parts
3	30	20	1	smooth, shallow, non-melted
4	30	20	3	smooth, enough depth, melted edges
5	40	30	7	smooth, 1/3 depth
6	40	30	9	smooth, 2/3 depth

Eventually, combination 6 was used for all hinges.

7.4 Setup Fabrication Details

In figure 37 the design of the SMP clamp can be seen. The holes at the top are lasercut to secure the structure on the top beam, while at the bottom the screws will fix the SMP between the two

plates.In figure 38 an outline of the waterbox which has an outer dimension of 75x75x140mm and thickness of 4mm, is displayed.

Figure 37: Laser cut plexiglass in between which the SMP get clamped. The two plexiglass plates get secured on the sliding elements at the top and the SMP will be clamped at the bottom.

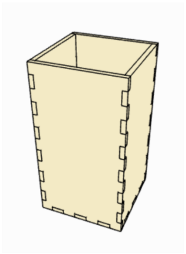

Figure 38: The waterbox in which the SMP will hang to be heated beyond its glass transition temperature for transition to flexible state.

7.5 Temperature experiments

Temperature experiments are done to investigate if there is any correlation between how far the SMP is heated above its glass transition temperature and the flexible state in which the SMP exists. From previous background information it can be concluded that there is a transition region between 20 and 60 degrees Celsius in which the elastic modulus of MP-3510 changes.

7.5.1 Method

When the temperature rises above the glass transition temperature of the SMP material, the substance becomes flexible. However it is questionable whether the ability to bend has any correlation with the temperature. For example if the temperature is closer to the transition point, is it then less flexible then if it surpasses it in larger amounts at higher temperatures? To investigate this, the temperature is set at 48 degrees Celsius and subsequently lowered by steps of three degrees. At each temperature the current through the PacMag is turned on, producing a magnetic field, where after the bending angle is measured with the camera. The magnetic field strength is set at a maximum of 45 mT in the x-direction for analysis and to meet dimensional requirements, two block magnet with dimensions 5x2x2mm were used throughout these experiments. The magnet was placed so that the north-pole was facing outwards and south-pole inwards in the x-direction, with the SMP panel facing to the left, like magnet 2a described in figure 12 but then facing to the left. By having the magnet orientated this way a magnetic field in the x-direction could be applied leading to only one possible rotations. This is because in the other direction the magnetic dipole is already aligned with the field.

7.5.2 Results

In figure 39, the average of the temperature experiments from three different tests is displayed. The results are not completely linear as can be seen from the trend line. However, there is an increase in maximal rotational angle when the water is at a higher temperature. The angles seem to decrease faster when below the glass transition temperature and increase slower when they are far above it. Predetermined, when the SMP was not stationed in water and the same magnetic field strength of 45 mT was applied, the rotational angle stayed at a constant 0 degrees. So the influence of the magnetic field strength solely of the magnets, without the SMP being in a flexible state, can be disregarded.

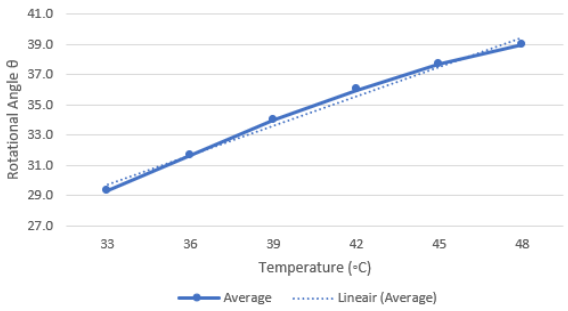

Figure 39: The figure portrays the Temperature Test. Every point indicating the average maximal angle measured at each water temperature at a maximal magnetic field strength of 45 mT.

7.6 Additional Results

7.6.1 Two Panel Experiments

Testing magnet a

The results for magnet a were only portrayed in the negative field direction due to greater rotation in this case. In figure 40 a comparison of the possible rotation is given, at the same field strength in the positive field versus the negative field.

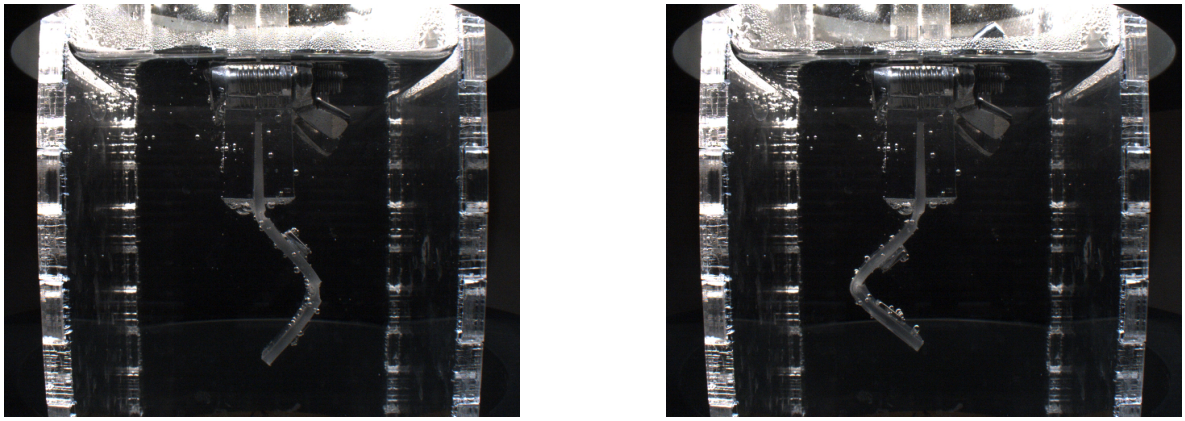

(a) Rotation of magnet a at 45mT.

(b) Rotation of magnet a at -45mT.

Figure 40: Rotation of magnet a during the two panel experiments in both the positive and negative field.

Testing magnet b

The results for magnet b are only given in the positive field because these were more distinctive. In figure 41 the results in the negative field direction are given.

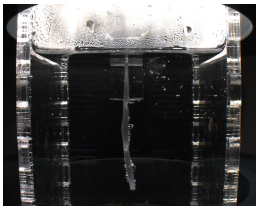

(a) Rotation of combination 1 at -45mT.

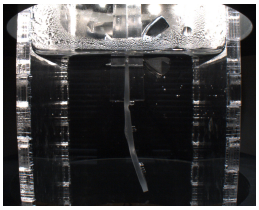

(b) Rotation of combination 2 at -45mT.

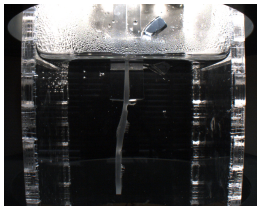

(c) Rotation of combination 3 at -45mT.

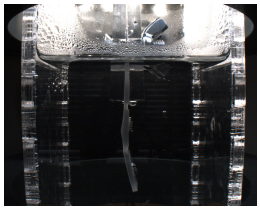

(d) Rotation of combination 4 at -45mT.

Figure 41: Rotation of magnets at a constant magnetic field strength in the x-direction. The red arrow indicates the direction of the magnetic moment vector and blue the direction of the magnetic field.

7.6.2 Four Panel Experiments

Testing magnet a

In the four panel experiments only the results for magnet a in the negative field direction were given. In figure 42 the results in the positive field can be found.

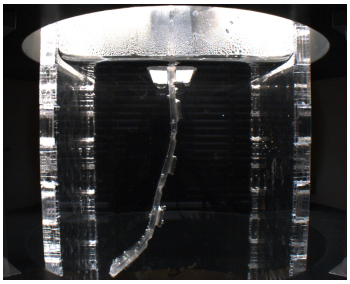

(a) Zigzag for combination 1.

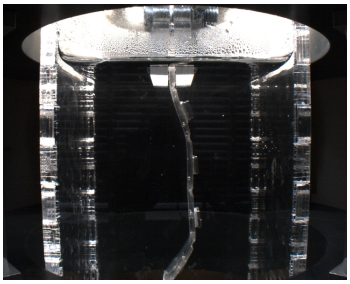

(b) Zigzag for combination 2.

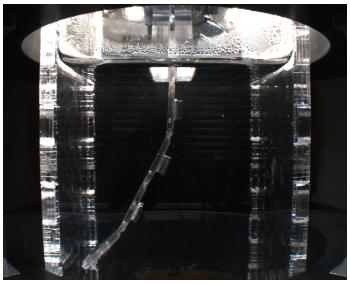

(c) Zigzag for combination 3.

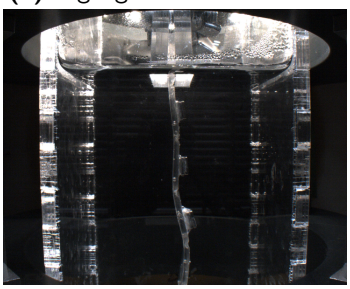

(d) Zigzag for combination 4.

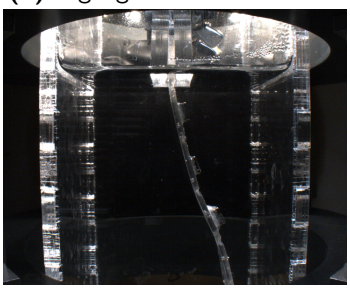

(e) Zigzag for combination 5.

Figure 42: Rotation of magnets on all panels at a constant magnetic field strength in the positive z-direction. The red arrow indicates the direction of the magnetic moment vector and blue the direction of the magnetic field.